Ahmed MA, Tsimenidis C, Al Rawi AF.

Performance Analysis of Full-Duplex-MRC-MIMO with Self-interference Cancellation Using Null-Space-Projection.

Transactions on Signal Processing

2016, 64(12), 3093-3105

Performance Analysis of Full-Duplex-MRC-MIMO With Self-Interference Cancellation Using Null-Space-Projection

Mohamad A. Ahmed, *Student Member, IEEE*, Charalampos C. Tsimenidis, *Senior Member, IEEE*, and Anas F. Al Rawi, *Member, IEEE*

***Abstract*—In this paper, the performance analysis of a full-duplex maximum ratio combining multiple-input multiple-output (FD-MRC-MIMO) system based on equalize-and-forward (EF) relaying with self-interference-cancellation (SIC) is derived under imperfect channels state information (CSI). The performance of the system is investigated in the presence of additive white Gaussian noise (AWGN) over Rayleigh fading channels. Self-interference cancellation is performed by applying null-space-projection (NSP) via singular-value-decomposition (SVD). Furthermore, exact, closed-form solutions for the signal-to-interference-plus-noise ratio (SINR) distribution and outage probability are mathematically formulated and evaluated along with the average symbol-error-rate (ASER) for M-ary phase-shift keying (M-PSK) modulation. The coefficients of the EF-relay are obtained to attain the minimum mean square error (MMSE) between the transmission symbols. Comparison of the obtained results with relevant state-of-the-art techniques suggests significant improvements in the SINR figures and system capacity.**

***Index Terms*—Full-duplex (FD), maximum ratio combining (MRC), multiple-input-multiple-output (MIMO), self-interference-cancellation (SIC), equalize-and-forward (EF), null-space-projection (NSP), singular-value-decomposition (SVD).**

I. Introduction

DUE to the continually increasing demands on frequency and energy resources, full-duplex (FD) has become an essential necessity and inevitable evolutionary step in the realm of wireless communications. FD transceivers allow transmission simultaneously over similar frequency bands. However, one of the key challenges in full-duplex wireless communication is the self-interference (SI), sometimes referred to as loop-interference (LI) too, that might affect undesirably to the overall system performance. This is principally caused by the transmitted signals of the FD transceiver, which exhibit larger energy than the desired incoming signals due to path loss propagation phenomena. The large power differential between the signal of interest which arrives weak from an away source and the self-interference signal created by the FD transceiver itself poses extreme difficulties to the receiver that needs to reconstruct and detect the desired signal.

This research paper focuses on FD-MIMO based relays, over which the source and destination nodes are communicating. The relay has the ability to receive data from the source and deliver it to the destination either by using amplify-and-forward (AF), decode-and-forward (DF), or by equalize-and-forward (EF) approaches. For these types of relaying, estimation and subtraction operations of SI are required to maximize the signal-to-interference-plus-noise ratio (SINR), which increases the capacity, improves the overall spectral efficiency and enhances the entire performance of these systems utilizing the FD technique. Thus far, several methods have been proposed in this field to mitigate SI that can be grouped in two categories, namely passive and/or active self-interference cancellation (SIC). Passive methods rely on separation between transmit and receive antennas in order to increase the isolation loss amongst them, and hence, reduce the magnitude of the local interference. In contrast, active approaches are implemented either in analogue domain, which is always before the analog-to-digital converter (ADC), or in digital domain, thus after the ADC. This can be accomplished by obtaining precise knowledge of the interfering signal and its channel and subtracting it either in passband or baseband, respectively. Furthermore, a combination between different domain methods can be used to obtain better performance.

In order to suppress SI in FD systems, it is initially required to reduce the effects of local power coupling to avoid *drowning* of the desired incoming signal in loop-interference, which is significantly stronger, and *mitigate* saturation of ADC circuitry due to limited dynamic range and quantization resolution [1]–[6]. Thus, passive suppression has been proposed at the receiver front-end by using natural-isolation (NI) techniques, or sometimes called passive-suppression (PS), via antenna separation to diminish and block the line-of-sight (LoS) path. This is achieved by orienting transmit antenna elements to an opposite direction than those of the receiving antennas, which consequently maximizes LI attenuation by increasing the insertion loss that can be

Manuscript received April 09, 2015; revised September 25, 2015, December 25, 2015, and February 24, 2016; accepted February 25, 2016. Date of publication March 10, 2016; date of current version April 21, 2016. The associate editor coordinating the review of this manuscript and approving it for publication was Prof. Walaa Hamouda. This work was supported by the EPSRC under project EP/N004299/1, Cooperative Backhaul Aided Next-Generation Digital Subscriber Loops.

M. A. Ahmed is with the School of Electrical and Electronic Engineering, Newcastle University, Newcastle upon Tyne, NE1 7RU, U.K., and also with the Electronics Engineering College, University of Mosul, Mosul 41002, Iraq (e-mail: m.a.ahmed2@newcastle.ac.uk; mohamad.alhabbar@uomosul.edu.iq).

C. C. Tsimenidis is with the School of Electrical and Electronic Engineering, Newcastle University, Newcastle upon Tyne NE1 7RU, U.K. (e-mail: charalampos.tsimenidis@newcastle.ac.uk).

A. F. Al Rawi is with the Research Department of British Telecom (BT), Martlesham Heath, IP5 3RE, U.K. (e-mail: anas.mohsin@bt.com).

Color versions of one or more of the figures in this paper are available online at http://ieeexplore.ieee.org.

Digital Object Identifier 10.1109/TSP.2016.2540611

further increased by utilizing orthogonal polarization schemes [2], [7]–[10].

Passive SI reduction can be used in conjunction with active suppression approaches that exploit local knowledge of transmitted data and loop channel information to remove SI. The latter needs to be accurately estimated in order to successfully mitigate it [2]. One conventional SIC method used in this area is based on the idea of utilizing the known transmitted data along with the estimated loop channel to reconstruct the interference signal and subtract it from the received signals. This scheme is referred to as time-domain cancellation (TDC) [2], [7], [11].

Spatial suppression schemes for FD-MIMO transceivers, such as zero-forcing (ZF) and null-space projection (NSP), are proposed as SIC via exploiting the spatial domain MIMO signal characteristics of the interfering channels. This can be achieved by designing spatial filters via utilizing matrix conversion approaches, as singular-value-decomposition (SVD) of the SI channel required to suppress the SI [2], [7], [11]–[13].

In contrast, in order to increase the signal to noise ratio (SNR), spatial diversity can be exploited for MIMO systems to obtain the full diversity gain available, which can be achieved by utilizing maximum ratio combining (MRC). This approach has been launched and deployed successfully for MIMO systems that operate in the presence of additive white Gaussian noise (AWGN) and interference environments. The MIMO-MRC system may be constructed by introducing transmit and receive beamforming weight vectors. The selection of beamforming weight vectors can be optimized to satisfy transmitting the signal over the strongest path of the channel. This implies that transmitting the signal along the direction of the eigenvector associated to the largest eigenvalue of the Wishart matrix of a channel $\mathbf{H}$, i.e., $\mathbf{H}^H\mathbf{H}$ [14], [15]. However, perfect channel state information (CSI) is required by the transmitter and receiver in order to obtain better performance.

Cooperative communications utilizing either AF, DF or EF relaying, have recently gained increased attention for their potential to enhance spectral efficiency and channel capacity, and to extend wireless coverage. In [5], the achievable rates under limited transmit/receive dynamic range for DF relaying utilizing FD-MIMO are studied in the presence of channel estimation errors. The authors propose maximization of the end-to-end (E2E) lower bound achievable rate based on a transmission scheme that requires solving a nonconvex optimization problem. In [16], the overall capacity of a FD-MIMO system based on AF relaying is presented using an optimal transformation matrix that maximizes the mutual information under average power constraint at the relay output under the assumption of perfect channel estimation. The latter work extends the results obtained in [17] from single-input single-output (SISO) to MIMO communication. An alternative half-duplex (HD) design is presented in [18], in which an AF relaying cooperative linear transceiver is analyzed under perfect source-to-destination CSI aided with an applied optimization routine to maximize the mutual information of the transmission system.

In this paper, we extend the works in [2], [7], [11]–[13] by combining MRC with NSP for FD-MIMO based relaying in order to maximize the SINR. Additionally, we derive the performance analysis of the proposed system for different performance metrics and in the presence of perfect and imperfect channel estimation. Furthermore, we extend the works in [5], [16]–[18] by utilizing EF relaying instead of DF and AF relays and we derive the relay transformation coefficients for FD-MRC-MIMO using EF relaying in order to minimize the mean square error (MSE) between the transmitted and the received symbols. Moreover, the E2E performance is demonstrated using the outage probability, average symbol error rate (ASER) vs. SINR, and capacity performance metrics.

The key contributions of this paper can be summarized as follows. Firstly, null-space-projection (NSP) and MRC are exploited jointly in order to mitigate the SI of the undesired loop path and to increase the SNR of the source-to-destination path. The motivation to use MRC-MIMO, which is selected over Full-MIMO, is due to the SNR advantage inherent in transmit and receive beamforming to achieve full diversity gain in such an interference limited environment. NSP is implemented via utilizing SVD of the CSI of the SI channel. Secondly, the E2E performance analysis of the modelled system takes into account the impact of imperfectly estimated CSI for both the desired and interference channels. Finally, the E2E upper bound mutual information of the proposed FD-MRC-MIMO is derived in the presence of SI. To the best of our knowledge, these aspects have not been thoroughly investigated in previously published research papers. The ideas, derivations and numerical results presented in this paper are valid for flat fading channels. However, the latter condition can be always satisfied by introducing orthogonal frequency division multiplex (OFDM) to combat intersymbol interference (ISI). As long as a cyclic prefix of sufficient length is selected to cover the delay spread of the multipath channel the presented results will be valid.

The rest of the paper is organized as follows. In Section II, the signal and system models are introduced. In Section III, we demonstrate the E2E performance analysis of the proposed system by deriving the output SINRs for the first and second hops along with their corresponding probability density functions (PDF). Furthermore, we derive the outage probabilities and ASER. In Section IV, the E2E upper bound capacity of this system is derived. Section V presents simulation results and discussion, and finally, the paper's conclusions are drawn in Section VI.

Notation: Matrix and vectors are denoted by uppercase and lowercase boldface characters, respectively. The transpose, conjugate and Hermitian of matrix $\mathbf{A}$ are denoted by $\mathbf{A}^T$, $\mathbf{A}^*$ and $\mathbf{A}^H$, respectively. $\|\mathbf{a}\|$, $\|\mathbf{A}\|$, are the Euclidean norm of the vector $\mathbf{a}$ and the matrix $\mathbf{A}$, respectively, while, $|\mathbf{A}|$ is the determinant of the matrix $\mathbf{A}$. Also $\Gamma(a)$ is the complete Gamma function of variable a. $\mathbb{E}(\mathbf{x})$ is the statistical expectation of the random vector $\mathbf{x}$. Finally, the binomial coefficient is defined as $\binom{a}{b} = \frac{a!}{b!(a-b)!}$ where $a!$ is the factorial of a. $\Re[A]$ and $\Im[A]$ represent for the real and imaginary parts of A, respectively.

II. Signal and System Model

In this paper, a wireless communications system is considered in which the source communicates with destination via relay as shown in Fig. 1, in addition to the description and definition mentioned in Table I. The relay operates as a full-duplex EF

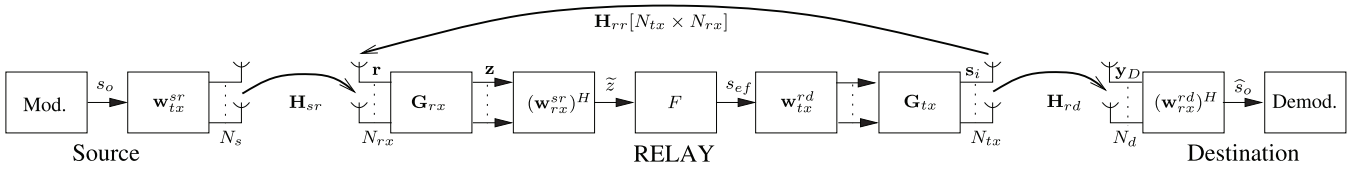

Fig. 1. Full-Duplex MRC-MIMO system with self-interference cancellation.

TABLE I
MODEL PARAMETERS

Notation	Description/Definition
	Source-Relay Parameters
s_o	Modulated symbol
$\mathbf{w}_{tx}^{sr}$	MRC weighting coefficients for transmitting with respect to $\mathbf{H}_{sr}$
$\mathbf{H}_{sr}$	source-relay channel coefficients
	Relay Parameters
$\mathbf{r}$	Sum of the received signal from the source coupled with $\mathbf{s}_i$ over $\mathbf{H}_{rr}$
$\mathbf{G}_{rx}$	Spatial filter determined by the first unitary matrix of SVD($\mathbf{H}_{rr}$)
$\mathbf{z}$	Output of the filter $\mathbf{G}_{rx}$
$(\mathbf{w}_{rx}^{sr})^H$	MRC weighting coefficients for detection with respect to $\mathbf{H}_{sr}$
$\widetilde{z}$	Weight received symbol
F	MMSE coefficient of the EF-relay
s_{ef}	Output of F
$\mathbf{w}_{tx}^{rd}$	MRC weighting coefficients for transmitting with respect to $\mathbf{H}_{rd}$
$\mathbf{G}_{tx}$	Spatial filter determined by the second unitary matrix of SVD($\mathbf{H}_{rr}$)
$\mathbf{s}_i$	Transmitted symbols from relay to destination
$\mathbf{H}_{rd}$	Relay to destination Channel
$\mathbf{H}_{rr}$	Self-interference Channel
	Relay-Destination Parameters
$\mathbf{y}_D$	The Received signal at the destination
$(\mathbf{w}_{rx}^{rd})^H$	MRC weighting coefficients for detection with respect to $\mathbf{H}_{rd}$
$\hat{s}_o$	The received symbol at the destination after applying MRC to $\mathbf{y}_D$

transceiver with N_{tx} transmit and N_{rx} receive antennas. Furthermore, the source has N_s antennas used to send the signal, while, N_d antennas at the destination are used for receiving. The channels between the source and the relay, the relay-to-destination, and the relay output to its input are considered in this paper as flat Rayleigh fading channels and they are defined as $\mathbf{H}_{sr} \sim \mathcal{CN}(\mathbf{0}, \mathbf{I}^{N_s \times N_{rx}}), \mathbf{H}_{rd} \sim \mathcal{CN}(\mathbf{0}, \mathbf{I}^{N_{tx} \times N_d})$, and $\mathbf{H}_{rr} \sim \mathcal{CN}(\mathbf{0}, \mathbf{I}^{N_{tx} \times N_{rx}})$, respectively. The assumption that the $\mathbf{H}_{rr}$ links are flat comes from the fact that passive suppression of SI has been implemented in the analogue domain via antenna separation and shielding to suppress the line-of-sight (LoS) paths [2]. In addition, AWGN is defined generally as $\mathbf{n} \sim \mathcal{CN}(\mathbf{0}, \sigma_n^2\mathbf{I})$. In this paper, we assume that there is no directly available source-to-destination path, i.e., $\mathbf{H}_{sd} = \mathbf{0}$, and all E2E communications occurs via the relay.

As highlighted in the Introduction Section, the FD-MRC-MIMO system applies transmit and receive beamforming at the source terminal and relay, respectively. The weight vectors at both transmitter and receiver are designed to maximize the SNR of the desired path by exploiting the eigen-transmissions and providing full diversity gain [14], [15]. This consequently leads to improved SINR for fixed SI and noise power levels ([19], p. 230–233). This can be obtained by using $\mathbf{w}_{tx}^{sr} = \mathbf{u}_{\max}^{sr}$ as MIMO transmit beamforming and $\mathbf{w}_{rx}^{sr} = \mathbf{H}_{sr}\mathbf{u}_{\max}^{sr}$ at the receiver as MRC reception, where $\mathbf{u}_{\max}^{sr}$ is the a unit norm eigenvector corresponding to the largest eigenvalue $\lambda_{\max}^{sr}$ of the Wishart matrix $\mathbf{H}_{sr}^H\mathbf{H}_{sr}$, where unit norm implies that the Euclidean norm of $\mathbf{u}_{\max}^{sr}$ is unity, i.e., $\|\mathbf{u}_{\max}^{sr}\|^2 = 1$. This is due to the fact that maximizing SNR is subject to determining the squared-spectrum norm of the matrix $\mathbf{H}_{sr}$, which suggests that the signal is transmitted from source-to-relay over the strongest path of $\mathbf{H}_{sr}$ [14], [15]. The same procedure can be used in the path of relay-to-destination of $\mathbf{H}_{rd}$ to obtain $\mathbf{w}_{tx}^{rd}$ and $\mathbf{w}_{rx}^{rd}$.

This research focuses on FD-MIMO based relay systems, which offer additional degrees of freedom in the spatial domain [2]. Spatial suppression schemes have been proposed and applied extensively for this issue. This is achieved by adding a receive filter, $\mathbf{G}_{rx} \in \mathbb{C}^{N_{rx} \times N_{rx}}$, at the input of the FD relay, and a transmit filter, $\mathbf{G}_{tx} \in \mathbb{C}^{N_{tx} \times N_{tx}}$, at the output of relay, as illustrated in Fig. 1. Both of these filters are designed based as eigen-beamformers using the SVD of the SI channel of the relay, $\mathbf{H}_{rr}$, with $\mathbf{H}_{rr} = \mathbf{U}_{rr}\mathbf{\Sigma}_{rr}\mathbf{V}_{rr}^H$, where $\mathbf{U}_{rr} \in \mathbb{C}^{N_{rx} \times N_{rx}}$ and $\mathbf{V}_{rr} \in \mathbb{C}^{N_{tx} \times N_{tx}}$ are unitary matrices, i.e., $\mathbf{U}_{rr}\mathbf{U}_{rr}^H = \mathbf{U}_{rr}^H\mathbf{U}_{rr} = \mathbf{I}$ and $\mathbf{V}_{rr}\mathbf{V}_{rr}^H = \mathbf{V}_{rr}^H\mathbf{V}_{rr} = \mathbf{I}$. Here, $\mathbf{U}_{rr}$ and $\mathbf{V}_{rr}$ are constructed using orthogonal column vectors of $\mathbf{H}_{rr}$. In addition, $\mathbf{\Sigma}_{rr} \in \mathbb{R}^{N_{rx} \times N_{tx}}$ is a diagonal matrix containing in descending order the singular values, $\sigma_{rr}[i] \geq 0$, for $i = 1, 2, \ldots, \min\{N_{rx}, N_{tx}\}$ of $\mathbf{H}_{rr}$ [7], [11].

The target in designing the filters from the SVD of the SI channel is to obtain $\mathbf{G}_{rx}\mathbf{H}_{rr}\mathbf{G}_{tx} = \mathbf{0}$, which is referred to as NSP. However, the channel estimation error will cause residual SI, which impacts negatively on the overall performance of the system. In order to design $\mathbf{G}_{rx}$ and $\mathbf{G}_{tx}$, there are several approaches that can be utilized as in [2], [7], [11], [13], [20]–[23]. As the emphasis of this paper is on the performance analysis of SI of FD-MIMO relays in the presence of SIC, we have used the approach outlined in [13] and [22], which is suitable for MIMO systems with the same number of transmit and receive antennas, i.e., $N_{rx} = N_{tx}$. In this method, the two spatial filters are designed by selecting one of the two options in (1) in order to satisfy $\min \|\mathbf{G_{tx}}\mathbf{H_{rr}}\mathbf{G_{rx}}\|_F^2$ [2], i.e.,

$$\mathbf{G}_{rx} = [\mathbf{u}_{rr}^{(0)} \quad \mathbf{u}_{rr}^{(0)}]^H, \quad \text{if } \mathbf{G}_{tx} = [\mathbf{v}_{rr}^{(1)} \quad \mathbf{v}_{rr}^{(1)}], \tag{1a}$$

$$\mathbf{G}_{rx} = [\mathbf{u}_{rr}^{(1)} \quad \mathbf{u}_{rr}^{(1)}]^H, \quad \text{if } \mathbf{G}_{tx} = [\mathbf{v}_{rr}^{(0)} \quad \mathbf{v}_{rr}^{(0)}], \tag{1b}$$

where $\mathbf{u}_{rr}^{(0)}$ and $\mathbf{v}_{rr}^{(0)}$ represent the first half columns of the matrices $\mathbf{U}_{rr}$ and $\mathbf{V}_{rr}$, respectively, while, $\mathbf{u}_{rr}^{(1)}$ and $\mathbf{v}_{rr}^{(1)}$ represent the second half columns of matrices $\mathbf{U}_{rr}$ and $\mathbf{V}_{rr}$ respectively. In addition, for non-square matrices and/or for the case of rank deficiency of $\mathbf{H}_{rr}$, (2) from [21] might be used to design the two filters as

$$\mathbf{G}_{rx} = \mathbf{U}_{rr}^H(:, \text{rank}(\mathbf{H}_{rr}) + 1 : N_{rx}), \tag{2a}$$

$$\mathbf{G}_{tx} = \mathbf{V}_{rr}(:, \text{rank}(\mathbf{H}_{rr}) + 1 : N_{tx}), \tag{2b}$$

where $\text{rank}(\mathbf{H}_{rr})$ represents the rank of $\mathbf{H}_{rr}$.

In Fig. 1, F represents the minimum mean square error (MMSE) transformation coefficient of the EF-relay, which is derived in detail in Appendix B in order to obtain the optimum solution that minimizes the errors between the transmitted and the received symbols in the source-to-relay path in the presence

of residual SI, and therefore, enhances the overall performance of the system.

III. E2E Performance Analysis

In this section, the E2E performance analysis is derived. The derivation is organized as follows; we derive the SINR, PDF of the output SINR, the outage probability, and the ASER for the first and second hops in Subsections III.A and III.B, respectively. The overall probability of error for the entire system can be obtained as [24]

$$P\{\mathbb{E}(\gamma_1,\gamma_2)\} = P_1\{\mathbb{E}(\gamma_1)\} + P_2\{\mathbb{E}(\gamma_2)\} - 2P_1\{\mathbb{E}(\gamma_1)\}P_2\{\mathbb{E}(\gamma_2)\}, \quad (3)$$

where $P\{\mathbb{E}(\gamma_1,\gamma_2)\}$ represents the E2E probability of error averaged over the two independent random variables γ_1 and γ_2, which represent the SINRs of the first and second hops, respectively, whilst, in general, $P_i\{\mathbb{E}(\gamma_i)\}, i \in \{1,2\}$ represents the average probability of error over the independent random variable γ_i.

A. SINR of the First Hop

The focus of this paper is on the full-duplex relay that can send and receive data simultaneously, which in turn causes SI in the receive terminal. Thus, in this section, the SINR is derived for the first hop of the modelled system. For a given MIMO symbol and at time instant t, the received signal vector, $\mathbf{r}[t]$, at the FD-MRC-MIMO relay input can be written as

$$\mathbf{r}[t] = \sqrt{P_{sr}}\mathbf{H}_{sr}\mathbf{w}_{tx}^{sr}s_o[t] + \sqrt{P_{rr}}\mathbf{H}_{rr}\mathbf{s}_i\left(s_o[t-1]\right) + \mathbf{n}_R[t], \quad (4)$$

where $s_o[t] \in \exp(j(2k+1)\pi/M), \forall k = 0,\dots M-1$ represents the M-PSK symbols before applying a MIMO transmitter beamforming weight vector of the source to the relay path, $\mathbf{w}_{tx}^{sr}$. Whilst, $\mathbf{s}_i(s_o[t-1])$ is the relay's transmitted signal as a function of the previous transmitted symbol of the source, $s_o[t-1]$, i.e., it represents the raw transmitted symbols at the relay output after applying the EF relaying operation to $s_o[t-1]$. Additionally, P_{sr} and P_{rr} are the relay's average transmit powers from the forward path, i.e., the source-to-relay path, and the backward loop path of the relay causing SI, respectively. $\mathbf{n}_R[t]$ represents the AWGN at the input of the relay. Furthermore, in the following steps, we will assume that the processing delay in the EF relaying operation can be applied within a symbol duration.

The input for the relay EF processing stage, $\tilde{z}[t]$, is obtained by substituting $\mathbf{s}_i[t] = \mathbf{G}_{tx}\mathbf{w}_{tx}^{rd}s_{ef}[t-1]$ in (4), where s_{ef} represents the equalized complex symbol after passing through the MMSE transformation filter of the EF-relay, F. Then, by performing SIC processing of $\mathbf{r}[t]$ in the first stage of the EF-relay as $\mathbf{z}[t] = \mathbf{G}_{rx}\mathbf{r}[t]$, and applying the MRC weight vector at the relay as $\tilde{z}[t] = (\mathbf{w}_{rx}^{sr})^H\mathbf{z}[t]$, we can write

$$\begin{aligned}\tilde{z}[t] &= \sqrt{P_{sr}}(\mathbf{w}_{rx}^{sr})^H\mathbf{G}_{rx}\mathbf{H}_{sr}\mathbf{w}_{tx}^{sr}s_o[t] \\ &\quad + \sqrt{P_{rr}}(\mathbf{w}_{rx}^{sr})^H\underbrace{\mathbf{G}_{rx}\mathbf{H}_{rr}\mathbf{G}_{tx}}_{\text{SIC}}\mathbf{w}_{tx}^{rd}s_{ef}[t-1] \\ &\quad + (\mathbf{w}_{rx}^{sr})^H\mathbf{G}_{rx}\mathbf{n}_R[t], \end{aligned} \quad (5)$$

where the MRC weighted vectors are defined as $\mathbf{w}_{tx}^{sr} = \mathbf{u}_{\max}^{sr}, \mathbf{w}_{rx}^{sr} = \mathbf{H}_{sr}\mathbf{u}_{\max}^{sr}$, and $\mathbf{w}_{tx}^{rd} = \mathbf{u}_{\max}^{rd}$ for the case of perfect CSI.

It is obvious that SIC is achieved at this stage, however, imperfect channel estimation of the undesired channel, $\mathbf{H}_{rr}$, produces residual SI. In addition, the channel estimation error for the signal of interest, $\mathbf{H}_{sr}$, will impact the performance of the system. Therefore, this issue needs to be considered by adding the effect of channel estimation error as [25]

$$\mathbf{H}_{sr} = \sqrt{1-\epsilon_{sr}^2}\hat{\mathbf{H}}_{sr} + \epsilon_{sr}\Xi_{sr}, \quad (6a)$$

$$\mathbf{H}_{rr} = \sqrt{1-\epsilon_{rr}^2}\hat{\mathbf{H}}_{rr} + \epsilon_{rr}\Xi_{rr}, \quad (6b)$$

$$\mathbf{H}_{rd} = \sqrt{1-\epsilon_{rd}^2}\hat{\mathbf{H}}_{rd} + \epsilon_{rd}\Xi_{rd}, \quad (6c)$$

where $\hat{\mathbf{H}}_{sr} \sim \mathcal{CN}(0,\mathbf{I}^{N_s\times N_{rx}}), \hat{\mathbf{H}}_{rr} \sim \mathcal{CN}(0,\mathbf{I}^{N_{tx}\times N_{rx}})$ and $\hat{\mathbf{H}}_{rd} \sim \mathcal{CN}(0,\mathbf{I}^{N_{tx}\times N_d})$ represent channel estimates of $\mathbf{H}_{sr},\mathbf{H}_{rr}$ and $\mathbf{H}_{rd}$, respectively. Moreover $\Xi_{sr} \sim \mathcal{CN}(0,\mathbf{I}^{N_s\times N_{rx}}), \Xi_{rr} \sim \mathcal{CN}(0,\mathbf{I}^{N_{tx}\times N_{rx}})$ and $\Xi_{rd} \sim \mathcal{CN}(0,\mathbf{I}^{N_{tx}\times N_d})$ are the channel estimation errors of $\mathbf{H}_{sr},\mathbf{H}_{rr}$ and $\mathbf{H}_{rd}$, respectively, modelled as complex zero-mean Gaussian random variables with identity covariance matrices that are independent of their channels [25]. Furthermore, ϵ_{sr} and ϵ_{rr} are the channel estimation accuracies of $\hat{\mathbf{H}}_{sr}$ and $\hat{\mathbf{H}}_{rr}$, respectively, and in general they are defined as $\epsilon \in [0,1]$, which implies that when $\epsilon_{sr} = \epsilon_{rr} = 0$, the channels estimation is perfect. We can use $\rho_{sr} = \sqrt{1-\epsilon_{sr}^2}, \rho_{rr} = \sqrt{1-\epsilon_{rr}^2}$ and $\rho_{rd} = \sqrt{1-\epsilon_{rd}^2}$ to denote the effect of channel estimation errors in $\mathbf{H}_{sr},\mathbf{H}_{rr}$ and $\mathbf{H}_{rd}$, respectively. By substituting the effect of channel estimation error of (6) into (5), and applying the estimated MRC weighted vectors as $\mathbf{w}_{tx}^{sr} = \hat{\mathbf{u}}_{\max}^{sr}, \mathbf{w}_{rx}^{sr} = \hat{\mathbf{H}}_{sr}\hat{\mathbf{u}}_{\max}^{sr}$, and $\mathbf{w}_{tx}^{rd} = \hat{\mathbf{u}}_{\max}^{rd}, \tilde{z}[t]$ can be re-written as

$$\begin{aligned}&\tilde{z}[t] \\ &= \sqrt{1-\epsilon_{sr}^2}\sqrt{P_{sr}}(\hat{\mathbf{u}}_{\max}^{sr})^H\hat{\mathbf{H}}_{sr}^H\hat{\mathbf{G}}_{rx}\hat{\mathbf{H}}_{sr}\hat{\mathbf{u}}_{\max}^{sr}s_o[t] \\ &\quad + \epsilon_{sr}\sqrt{P_{sr}}(\hat{\mathbf{u}}_{\max}^{sr})^H\hat{\mathbf{H}}_{sr}^H\hat{\mathbf{G}}_{rx}\Xi_{sr}\hat{\mathbf{u}}_{\max}^{sr}s_o[t] \\ &\quad + \sqrt{1-\epsilon_{rr}^2}\sqrt{\tilde{P}_{rr}}(\hat{\mathbf{u}}_{\max}^{sr})^H\hat{\mathbf{H}}_{sr}^H\hat{\mathbf{G}}_{rx}\hat{\mathbf{H}}_{rr}\hat{\mathbf{G}}_{tx}\hat{\mathbf{u}}_{\max}^{rd}s_{ef}[t-1] \\ &\quad + \epsilon_{rr}\sqrt{\tilde{P}_{rr}}(\hat{\mathbf{u}}_{\max}^{sr})^H\hat{\mathbf{H}}_{sr}^H\hat{\mathbf{G}}_{rx}\Xi_{rr}\hat{\mathbf{G}}_{tx}\hat{\mathbf{u}}_{\max}^{rd}s_{ef}[t-1] \\ &\quad + (\hat{\mathbf{u}}_{\max}^{sr})^H\hat{\mathbf{H}}_{sr}^H\hat{\mathbf{G}}_{rx}\mathbf{n}_R[t], \end{aligned} \quad (7)$$

where $\hat{\mathbf{G}}_{rx}$ and $\hat{\mathbf{G}}_{tx}$ represent the MIMO receive and transmit filters, respectively, obtained from the SVD of estimated channel of SI, $\hat{\mathbf{H}}_{rr}$. It is important to note that $\tilde{P}_{rr}$ represents the residual power of SI after applying spatial cancellation via NSP. It can be observed that (7) contains the combination of the desired signal, noise, in addition to three terms of interferences, which are due to the SI channel of the FD-relay, and channel estimation errors of forward and backward loop path. Thus, the SINR of the first hop of the relay, γ_1, can be obtained from (7) as

$$\gamma_1 = \frac{(1-\epsilon_{sr}^2)P_{sr}\left\|(\hat{\mathbf{u}}_{\max}^{sr})^H\hat{\mathbf{H}}_{sr}^H\hat{\mathbf{G}}_{rx}\hat{\mathbf{H}}_{sr}\hat{\mathbf{u}}_{\max}^{sr}s_o[t]\right\|^2}{C_0+C_1+C_2+C_3}, \quad (8)$$

with

$$C_0 = \epsilon_{sr}^2P_{sr}\left\|(\hat{\mathbf{u}}_{\max}^{sr})^H\hat{\mathbf{H}}_{sr}^H\hat{\mathbf{G}}_{rx}\,\Xi_{sr}\hat{\mathbf{u}}_{\max}^{sr}s_o[t]\right\|^2, \quad (9a)$$

$$C_1 = (1-\epsilon_{rr}^2)\tilde{P}_{rr} \times \left\|(\hat{\mathbf{u}}_{\max}^{sr})^H \hat{\mathbf{H}}_{sr}^H \hat{\mathbf{G}}_{rx} \hat{\mathbf{H}}_{rr} \hat{\mathbf{G}}_{tx} \hat{\mathbf{u}}_{\max}^{rd} s_{ef}[t-1]\right\|^2, \quad (9b)$$

$$C_2 = \epsilon_{rr}^2 \tilde{P}_{rr} \left\|(\hat{\mathbf{u}}_{\max}^{sr})^H \hat{\mathbf{H}}_{sr}^H \hat{\mathbf{G}}_{rx}\, \Xi_{rr} \hat{\mathbf{G}}_{tx} \hat{\mathbf{u}}_{\max}^{rd} s_{ef}[t-1]\right\|^2, \quad (9c)$$

$$C_3 = \left\|(\hat{\mathbf{u}}_{\max}^{sr})^H \hat{\mathbf{H}}_{sr}^H \hat{\mathbf{G}}_{rx}\, \mathbf{n}_R[t]\right\|^2, \quad (9d)$$

where the term in the numerator of (8) represents the power of the desired signal. The denominator comprises four terms which are given in (9). The constant term C_0 represents the interference power due to channel estimation error of $\mathbf{H}_{sr}$, term C_1 represents the self-interference power of the channel $\mathbf{H}_{rr}$, term C_2 accounts for the power of interference caused by imperfect channel estimation of $\mathbf{H}_{rr}$, and finally, C_3 is for the noise power after passing through the MRC and SIC relay filters.

Equation (8) needs to be simplified in order to appreciate the contribution of the individual terms. To achieve this, firstly, we divide the numerator and denominator by $\|\hat{\mathbf{G}}_{rx}\|^2$. Secondly, since $\hat{\mathbf{u}}_{\max}^{sr}$ is the estimated eigenvector corresponding to the largest estimated eigenvalue $\hat{\lambda}_{\max}^{sr}$ of the Wishart matrix $\mathbf{H}_{sr}^H \mathbf{H}_{sr}$, it is constructive to compensate for $(\hat{\lambda}_{\max}^{sr})^2$ instead of $\left\|(\hat{\mathbf{u}}_{\max}^{sr})^H \hat{\mathbf{H}}_{sr}^H \hat{\mathbf{H}}_{sr} \hat{\mathbf{u}}_{\max}^{sr}\right\|^2$, and for $\hat{\lambda}_{\max}^{sr}$ instead of $\left\|(\hat{\mathbf{u}}_{\max}^{sr})^H \hat{\mathbf{H}}_{sr}^H\right\|^2$. Moreover, from the definitions of Ξ_{sr} and Ξ_{rr} following (6), we have $\mathbb{E}\{\|\Xi_{sr}\|^2\} = \mathbb{E}\{\|\Xi_{rr}\|^2\} = 1$ due to their unity-covariance [25]. Additionally, $\|\hat{\mathbf{u}}_{\max}^{sr}\|^2 = \left\|\hat{\mathbf{u}}_{\max}^{rd}\right\|^2 = 1$ as they represent the unit norm eigenvectors corresponding to the largest eigenvalues $\hat{\lambda}_{\max}^{sr}$ and $\hat{\lambda}_{\max}^{rd}$ of the estimated channels $\hat{\mathbf{H}}_{sr}$ and $\hat{\mathbf{H}}_{rd}$, respectively, as defined earlier in Section II. Moreover, variance of the noise is given as $E\left\{\|\mathbf{n}_R\|^2\right\} = \sigma_{n_R}^2$. By taking all these substitutions into account and after some additional straightforward mathematical manipulations, γ_1 can be rewritten as in (10) on the bottom of the page.

In (10), $\Omega_{sr} = P_{sr}/\sigma_{n_R}^2$ represents the SNR, while $\Omega_{rr} = \tilde{P}_{rr}/\sigma_{n_R}^2$ is the interference-to-noise ratio (INR) at the input of the MMSE transformation filter of the relay, F, after passive suppression and NSP cancellation. It can be noticed that (10b) represents the ratio of two independent random variables and can be re-written as

$$\gamma_1 = \frac{\alpha_{sr}\hat{\lambda}_{\max}^{sr}}{\frac{\beta}{\hat{\lambda}_{\max}^{sr}}\left\|(\hat{\mathbf{u}}_{\max}^{sr})^H \hat{\mathbf{H}}_{sr}^H \hat{\mathbf{H}}_{rr} \hat{\mathbf{G}}_{tx} \hat{\mathbf{u}}_{\max}^{rd}\right\|^2 + 1} \quad (11)$$

where

$$\alpha_{sr} = \frac{(1-\epsilon_{sr}^2)\Omega_{sr}}{\epsilon_{sr}^2\Omega_{sr} + \epsilon_{rr}^2\Omega_{rr} + 1}, \quad \beta = \frac{(1-\epsilon_{rr}^2)\Omega_{rr}}{\epsilon_{sr}^2\Omega_{sr} + \epsilon_{rr}^2\Omega_{rr} + 1}. \quad (12)$$

To gain insight on the relationship between SNR and SINR, we can re-write (12) as $\alpha_{sr} = \frac{(1-\epsilon_{sr}^2)}{\epsilon_{sr}^2 + \epsilon_{rr}^2(\Omega_{rr}/\Omega_{sr}) + 1/\Omega_{sr}}$ and $\beta = \frac{(1-\epsilon_{rr}^2)}{\epsilon_{sr}^2(\Omega_{sr}/\Omega_{rr}) + \epsilon_{rr}^2 + 1/\Omega_{rr}}$. The factor $\Omega_{sr}/\Omega_{rr} = P_{sr}/\tilde{P}_{rr}$ represents here the signal-to-interference ratio (SIR). Therefore, increasing the signal power for fixed levels of SI and noise power will cause α_{sr} to increase and β to decrease, which consequently results in an increase of γ_1 in (11).

1) Probability Density Function of γ_1: With return now our attention to (11). The SINR is considered as the ratio of two independent random variables x and y given by

$$\gamma_1 = \frac{y}{x+1}, \quad (13a)$$

$$x = \frac{\beta}{\hat{\lambda}_{\max}^{sr}}\left\|(\hat{\mathbf{u}}_{\max}^{sr})^H \hat{\mathbf{H}}_{sr}^H \hat{\mathbf{H}}_{rr} \hat{\mathbf{G}}_{tx} \hat{\mathbf{u}}_{\max}^{rd}\right\|^2, \quad (13b)$$

$$y = \alpha_{sr}\hat{\lambda}_{\max}^{sr}. \quad (13c)$$

Following the definitions in [15] and the derivations in [26], it is worth mentioning that the term $(\hat{\mathbf{u}}_{\max}^{sr})^H \hat{\mathbf{H}}_{sr}^H \hat{\mathbf{H}}_{rr} \hat{\mathbf{G}}_{tx} \hat{\mathbf{u}}_{\max}^{rd}/\hat{\lambda}_{max}^{sr}$ in (13b) is an independent and identically distributed (i.i.d.) complex Gaussian random variable, and it is independent of $\hat{\lambda}_{max}^{sr}$. This is due to the earlier assumption in Subsection III.A, that the estimated SI channel, $\hat{\mathbf{H}}_{rr}$, exhibits a circularly symmetric Gaussian distribution with zero mean and covariance matrix $\mathbf{I}^{N_{tx}\times N_{rx}}$. The mean of this term conditioned on $\hat{\mathbf{H}}_{sr}$ is derived as

$$\mathbb{E}\left[(\hat{\mathbf{u}}_{\max}^{sr})^H \hat{\mathbf{H}}_{sr}^H \hat{\mathbf{H}}_{rr} \hat{\mathbf{G}}_{tx} \hat{\mathbf{u}}_{\max}^{rd} \mid \hat{\mathbf{H}}_{sr}\right] = (\hat{\mathbf{u}}_{\max}^{sr})^H \hat{\mathbf{H}}_{sr}^H \underbrace{\mathbb{E}\left[\hat{\mathbf{H}}_{rr}\right]}_{\text{Mean}=0} \hat{\mathbf{G}}_{tx} \hat{\mathbf{u}}_{\max}^{rd} = 0, \quad (14)$$

while its variance conditioned on $\hat{\mathbf{H}}_{sr}$ can be derived as

$$\begin{aligned}\mathbb{E}\left[\left\|(\hat{\mathbf{u}}_{\max}^{sr})^H \hat{\mathbf{H}}_{sr}^H \hat{\mathbf{H}}_{rr} \hat{\mathbf{G}}_{tx} \hat{\mathbf{u}}_{\max}^{rd}\right\|^2 \mid \hat{\mathbf{H}}_{sr}\right] &= (\hat{\mathbf{u}}_{\max}^{sr})^H \hat{\mathbf{H}}_{sr}^H \underbrace{\mathbb{E}\left[\hat{\mathbf{H}}_{rr} \hat{\mathbf{G}}_{tx} \hat{\mathbf{G}}_{tx}^H \hat{\mathbf{H}}_{rr}^H\right]}_{\mathbf{I}^{N_{tx}\times N_{rx}}} \hat{\mathbf{H}}_{sr} \hat{\mathbf{u}}_{\max}^{sr} \\ &= (\hat{\mathbf{u}}_{\max}^{sr})^H \hat{\mathbf{H}}_{sr}^H \hat{\mathbf{H}}_{sr} \hat{\mathbf{u}}_{\max}^{sr} = \left\|(\hat{\mathbf{u}}_{\max}^{sr})^H \hat{\mathbf{H}}_{sr}^H\right\|^2 = \hat{\lambda}_{\max}^{sr}. \quad (15)\end{aligned}$$

$$\gamma_1 = \frac{(1-\epsilon_{sr}^2)\Omega_{sr}\lambda_{\max}^{sr}}{\frac{(1-\epsilon_{rr}^2)\Omega_{rr}}{\lambda_{\max}^{sr}}\left\|(\hat{\mathbf{u}}_{\max}^{sr})^H \hat{\mathbf{H}}_{sr}^H \hat{\mathbf{H}}_{rr} \hat{\mathbf{G}}_{tx} \hat{\mathbf{u}}_{\max}^{rd}\right\|^2 + \epsilon_{sr}^2\Omega_{sr} + \epsilon_{rr}^2\Omega_{rr} + 1}, \quad (10a)$$

$$= \frac{\frac{(1-\epsilon_{sr}^2)\Omega_{sr}\lambda_{\max}^{sr}}{(\epsilon_{sr}^2\Omega_{sr} + \epsilon_{rr}^2\Omega_{rr} + 1)}}{\frac{(1-\epsilon_{rr}^2)\Omega_{rr}}{\lambda_{\max}^{sr}(\epsilon_{sr}^2\Omega_{sr} + \epsilon_{rr}^2\Omega_{rr} + 1)}\left\|(\hat{\mathbf{u}}_{\max}^{sr})^H \hat{\mathbf{H}}_{sr}^H \hat{\mathbf{H}}_{rr} \hat{\mathbf{G}}_{tx} \hat{\mathbf{u}}_{\max}^{rd}\right\|^2 + 1}. \quad (10b)$$

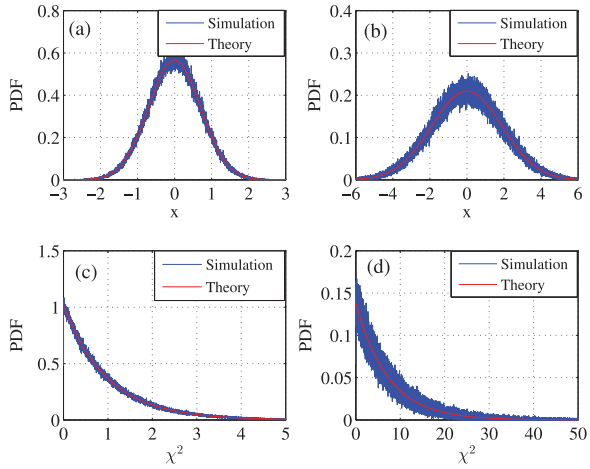

Fig. 2. The PDF of $\Re\left\{(\hat{\mathbf{u}}_{\max}^{sr})^H \hat{\mathbf{H}}_{sr}^H \hat{\mathbf{H}}_{rr} \hat{\mathbf{G}}_{tx} \hat{\mathbf{u}}_{\max}^{rd}\right\}$ in (a) and (b), while the PDF of $\left|\left|(\hat{\mathbf{u}}_{\max}^{sr})^H \hat{\mathbf{H}}_{sr}^H \hat{\mathbf{H}}_{rr} \hat{\mathbf{G}}_{tx} \hat{\mathbf{u}}_{\max}^{rd}\right|\right|^2$ in (c) and (d), for $\hat{\lambda}_{max}^{sr} = 0.7$ and 1.9.

A closer look into (15) reveals that its first equality contains two independent random variables which are $\hat{\mathbf{H}}_{rr}\hat{\mathbf{G}}_{tx}$ and $\hat{\mathbf{u}}_{max}^{rd}$. As defined earlier in Section II, we can substitute for $\left\|\hat{\mathbf{u}}_{\max}^{rd}\right\|^2 = \left\|\hat{\mathbf{u}}_{\max}^{rd}(\hat{\mathbf{u}}_{\max}^{rd})^H\right\| = 1$. Moreover, the expectation for the first random variable can be substituted by the identity matrix $\mathbf{I}^{N_{tx}\times N_{rx}}$, as the SI channel, $\hat{\mathbf{H}}_{rr}$, is an i.i.d. Rayleigh distributed random variable containing i.i.d. complex Gaussian vectors with zero-mean and covariance matrix $\mathbf{I}^{N_{tx}\times N_{rx}}$. Additionally, $\hat{\mathbf{G}}_{tx}$ is a matrix such that $\mathbb{E}\left[\hat{\mathbf{H}}_{rr}\hat{\mathbf{G}}_{tx}\hat{\mathbf{G}}_{tx}^H\hat{\mathbf{H}}_{rr}^H\right] = \mathbf{I}^{N_{tx}\times N_{rx}}$.

In Fig. 2(a) and (b), we illustrate the empirical (histogram) and theoretical distributions of the real part of (13b) for $N_{rx} = N_{tx} = 2$, and for two different values of $\hat{\lambda}_{max}^{sr}$, i.e., 0.7 and 1.9, respectively. It is worth noting, that due to symmetry, the distribution of the imaginary part follows a similar distribution. Since the $(\hat{\mathbf{u}}_{\max}^{sr})^H\hat{\mathbf{H}}_{sr}^H\hat{\mathbf{H}}_{rr}\hat{\mathbf{G}}_{tx}\hat{\mathbf{u}}_{\max}^{rd}$ is a complex, zero-mean, Gaussian random variable with variance $\hat{\lambda}_{max}^{sr}$, its norm will follow a Chi-squared distribution with N_{rx} degree of freedom ([27], p. 45). Fig. 2(c) and (d) demonstrate the Chi-squared distribution assumption for the variable $||(\hat{\mathbf{u}}_{\max}^{sr})^H\hat{\mathbf{H}}_{sr}^H\hat{\mathbf{H}}_{rr}\hat{\mathbf{G}}_{tx}\hat{\mathbf{u}}_{\max}^{rd}||^2$ for the two values of $\hat{\lambda}_{max}^{sr} = 0.7$ and 1.9, respectively.

The relationship of those two variables in (13b) and (13c) along with their scale factors in (12) follow the Gamma distribution [15]. Therefore, the PDF of $x, p_x(x)$, which can be denoted in general as $\mathcal{G}(x;j;\beta) = \frac{1}{\Gamma(j)}x^{j-1}\beta^{-j}e^{-x/\beta}$ [14], [28], exhibits a shape factor $(j = 1)$ due to the fact that only one source of SI is present by assumption and the scale factor, β, which leads us to

$$p_x(x) = \frac{1}{\beta}e^{\frac{-x}{\beta}}. \tag{16}$$

In constrast, $p_y(y)$ can be given as

$$p_y(y) = \sum_{k=1}^{m}\sum_{l=n-m}^{(n+m-2k)k} c_{kl}\frac{1}{\Gamma(l+1)}y^l\left(\frac{k}{\alpha_{sr}}\right)^{l+1} e^{-\frac{k}{\alpha_{sr}}y}. \tag{17}$$

It is noticeable that the PDF of y follows the Gamma distribution as $\mathcal{G}(y;l+1;\alpha_{sr}/k) = \frac{1}{\Gamma(l+1)}y^l(\frac{k}{\alpha_{sr}})^{l+1}e^{-\frac{k}{\alpha_{sr}}y}$ [14], [28], with shape factor $(l+1)$ and the normalized scale factor of (α_{sr}/k). In (17), $m = \min\{N_s, N_{rx}\}$ and $n = \max\{N_s, N_{rx}\}$. The curve fitting coefficients, c_{kl}, of the PDF $p_y(y)$ have been determined and listed in tables for several combinations of transmit and receive antennas in [29]. Additionally, there exists a numerical method that has been proposed in [14] for the same purpose. Both approaches satisfy $\sum_{k=1}^{m}\sum_{l=n-m}^{(n+m-2k)k} c_{kl} = 1$.

After evaluating $p_x(x)$ in (16) and $p_y(y)$ in (17), the PDF of SINR of the first hop, $p_{\gamma_1}(\gamma_1)$, can be obtained by using integration as

$$p_{\gamma_1}(\gamma_1) = \int_{x=0}^{\infty}(1+x)p_y\left[(1+x)\gamma_1\right]p_x(x)dx. \tag{18}$$

This integration can be solved by exploiting the conversion of the term $(x+a)^n$ to a finite summation as $\sum_{k=0}^{n}\binom{n}{k}x^k a^{n-k}$ ([30], (1.111)). Subsequently, in order to obtain the final formula, it is required to compare the resulting equation with $\int_0^\infty x^{\nu-1}e^{-\mu x}dx = \mu^{-\nu}\Gamma(\nu)$ for positive $\mu > 0$ and $\nu > 0$ [30, (3.351.3)], i.e.,

$$p_{\gamma_1}(\gamma_1) = \sum_{k=1}^{m}\sum_{l=n-m}^{(n+m-2k)k}\sum_{r=0}^{l+1} c_{kl}\frac{\Gamma(r+1)}{\Gamma_1(l+1)}\binom{l+1}{r} \times\left(\frac{k}{\alpha_{sr}}\right)^{l+1}\frac{1}{\beta}\left(\frac{\alpha_{sr}\beta}{\alpha_{sr}+k\beta\gamma_1}\right)^{r+1}\gamma_1^l e^{-\frac{k}{\alpha_{sr}}\gamma_1}. \tag{19}$$

2) Outage Probability of γ_1: To evaluate the outage probability associated with the probability that γ_1 is less than the protection ratio of the threshold SINR [31], we compute $P_{\text{out}}(\gamma_{th}) \triangleq Pr\{\gamma_1 \le \gamma_{th}\} = \int_0^{\gamma_{th}} p_{\gamma_1}(\gamma_1)d\gamma_1$, or equivalently

$$P_{\text{out1}}(\gamma_{th}) = \int_{\gamma_1=0}^{\gamma_{th}}\int_{x=0}^{\infty}(1+x)\,p_y\left[(1+x)\gamma_1\right]\,p_x(x)\,dx\,d\gamma_1, \tag{20}$$

where $p_{\gamma_1}(\gamma_1)$ is determined by (18).

The integration in (20) might be simplified by exploiting the lower incomplete Gamma function. This can be achieved by using the formula $\gamma(n,x) = \int_0^x r^{n-1}e^{-r}dr = \Gamma(n)\left(1-e^{-x}\sum_{k=0}^{n-1}(x^k/k!)\right)$ for positive integers n, which is part of (20) ([30], (8.3521.1)). In addition, it is required to use the binomial term $(x+a)^n$ for $a = 1$, which has been previously defined in this section. The outage probability can be then expressed as

$$P_{\text{out1}}(\gamma_{th}) = \sum_{k=1}^{m}\sum_{l=n-m}^{(n+m-2k)k} c_{kl}\left[1-e^{-\frac{k\gamma_{th}}{\alpha_{sr}}} \times\sum_{r=o}^{l}\sum_{s=0}^{r}\frac{\Gamma(s+1)}{\Gamma(r+1)}\binom{r}{s}\left(\frac{1}{\beta}\right)\left(\frac{k\gamma_{th}}{\alpha_{sr}}\right)^r \times\left(\frac{\alpha_{sr}\beta}{\alpha_{sr}+k\beta\gamma_{th}}\right)^{s+1}\right]. \tag{21}$$

3) ASER for M-PSK Modulation Scheme for 1st Hop: In order to evaluate the exact ASER, $\bar{P}_e$, for any M-PSK modulation scheme, it is constructive to define the instantaneous SER $P_e(\gamma)$ for the scheme under consideration. Subsequently, by taking the expectation of SER over the instantaneous SINR, i.e., the mean of $P_e(\gamma)$ we obtain

$$\bar{P}_e(\gamma_1) = \mathbb{E}\left[P_e(\gamma_1)\right] = \int_0^{\infty} P_e(\gamma_1) p_{\gamma_1}(\gamma_1) d\gamma_1, \tag{22}$$

where $P_e(\gamma_1)$ can be defined with respect to Q-function as $P_e(\gamma_1) = aQ(\sqrt{2g\gamma_1})$, which is a general formula valid for several modulation schemes with a and g being modulation dependent constants. For instance, $(a = 1, g = 1)$ for BPSK, and $(a = 2, g \approx \sin^2(\pi/M))$ as acceptable approximated SER of M-PSK [32].

The ASER is derived for several modulation schemes in Appendix A to obtain the final expression as

$$\begin{aligned}\bar{P}_{e1} = \sum_{k=1}^{m} \sum_{l=n-m}^{(n+m-2k)k} \frac{a\, c_{kl}}{2} \Bigg[1 - \left(\frac{g\alpha_{sr}}{k}\right)^{\frac{1}{2}} \\ \times \frac{1}{\beta} \sum_{r=0}^{l} \sum_{s=0}^{r} \binom{2r}{r} \binom{r}{s} \left(\frac{1}{4}\right)^{r} \\ \times \Gamma(s+1) \left(1 + \frac{g\alpha_{sr}}{k}\right)^{s-r+\frac{1}{2}} \\ \times \Psi\left(s+1; s-r+\frac{3}{2}; \frac{1}{\beta}\left(1 + \frac{g\alpha_{sr}}{k}\right)\right)\Bigg]. \end{aligned} \tag{23}$$

B. SINR of the 2nd Hop

The second hop of this proposed system is assumed to be a conventional MRC-MIMO system, where the relay forwards the equalized signal after applying transmit beamforming, $\mathbf{w}_{tx}^{rd} = \mathbf{u}_{\max}^{rd}$, and the spatial filter, $\mathbf{G}_{tx}$. Therefore, the received signal vector at the destination can be written as

$$\mathbf{y}_D[t] = \sqrt{P_{rd}} \mathbf{H}_{rd} \mathbf{G}_{tx} \mathbf{w}_{tx}^{rd} s_{ef}[t-1] + \mathbf{n}_D[t], \tag{24}$$

where P_{rd} is the relay's average transmit power to the destination. By applying the MRC weighting vector, $\left(\mathbf{w}_{rx}^{rd}\right)^H$, to (24) we can obtain the $(t-1)$th time instant of $\hat{s}_o$ as

$$\begin{aligned}\hat{s}_o[t-1] = \sqrt{P_{rd}} (\mathbf{w}_{rx}^{rd})^H \mathbf{H}_{rd} \mathbf{G}_{tx} \mathbf{w}_{tx}^{rd} s_{ef}[t-1] \\ + \left(\mathbf{w}_{rx}^{rd}\right)^H \mathbf{n}_D[t], \end{aligned} \tag{25}$$

where $\left(\mathbf{w}_{rx}^{rd}\right)^H = \left(\mathbf{u}_{\max}^{rd}\right)^H \mathbf{H}_{rd}^H$ for the case of perfect CSI $\mathbf{H}_{rd}$. By considering the impact of imperfect CSI estimation of $\mathbf{H}_{rd}$ in (6c) and applying the estimated MRC weighted vectors as $\left(\mathbf{w}_{rx}^{rd}\right)^H = \left(\hat{\mathbf{u}}_{\max}^{rd}\right)^H \hat{\mathbf{H}}_{rd}^H$ and $\mathbf{w}_{tx}^{rd} = \hat{\mathbf{u}}_{\max}^{rd}$, we can re-write (25) as

$$\begin{aligned}\hat{s}_o[t-1] = \sqrt{1-\epsilon_{rd}^2}\sqrt{P_{rd}} \left(\hat{\mathbf{u}}_{\max}^{rd}\right)^H \hat{\mathbf{H}}_{rd}^H \hat{\mathbf{H}}_{rd} \hat{\mathbf{G}}_{tx} \hat{\mathbf{u}}_{\max}^{rd} s_{ef}[t-1] \\ + \epsilon_{rd}\sqrt{P_{rd}} \left(\hat{\mathbf{u}}_{\max}^{rd}\right)^H \hat{\mathbf{H}}_{rd}^H \Xi_{rd} \hat{\mathbf{G}}_{tx} \hat{\mathbf{u}}_{\max}^{rd} s_{ef}[t-1] \\ + (\hat{\mathbf{u}}_{\max}^{rd})^H \hat{\mathbf{H}}_{rd}^H \mathbf{n}_D[t]. \end{aligned} \tag{26}$$

It can be noticed that $\hat{s}_o[t-1]$ in (26) contains a combination of three terms, which are the desired signal, the channel estimation error term, and the noise, respectively. Therefore, the SINR of this path, γ_2, can be extracted for the second hop of the relay as

$$\gamma_2 = \frac{\left(1-\epsilon_{rd}^2\right) P_{rd} \left\| \left(\hat{\mathbf{u}}_{\max}^{rd}\right)^H \hat{\mathbf{H}}_{rd}^H \hat{\mathbf{H}}_{rd} \hat{\mathbf{G}}_{tx} \hat{\mathbf{u}}_{\max}^{rd} s_{ef}[t-1] \right\|^2}{C_4 + C_5}, \tag{27}$$

where

$$C_4 = \epsilon_{rd}^2 P_{rd} \left\| \left(\hat{\mathbf{u}}_{\max}^{rd}\right)^H \hat{\mathbf{H}}_{rd}^H \Xi_{rd} \hat{\mathbf{G}}_{tx}\, \hat{\mathbf{u}}_{\max}^{rd} s_{ef}[t-1] \right\|^2, \tag{28a}$$

$$C_5 = \left\| \left(\hat{\mathbf{u}}_{\max}^{rd}\right)^H \hat{\mathbf{H}}_{rd}^H \mathbf{n}_D[t] \right\|^2. \tag{28b}$$

It is worth mentioning that C_4 represents the interference power due to channel estimation error of $\mathbf{H}_{rd}$ and C_5 is for the noise power after passing through the MRC stage of the destination node. In order to simplify (27), we can apply the similar simplifications and substitutions applied previously to (8) in Subsection III.A in order to re-write (27) as

$$\gamma_2 = \alpha_{rd} \lambda_{\max}^{rd}, \tag{29}$$

where

$$\alpha_{rd} = \frac{(1-\epsilon_{rd}^2)\Omega_{rd}}{\epsilon_{rd}^2 \Omega_{rd} + 1}, \tag{30}$$

where $\Omega_{rd} = P_{rd}/\sigma_{n_D}^2$ represents the SNR of the second hop.

1) PDF of γ_2: Unlike (11), the SINR of the second hop in (29) depends on one random variable. Thus, compared to (13c), we can employ (17) to evaluate the PDF of the output SINR of the second hop, $p_{\gamma_2}(\gamma_2)$ as

$$p_{\gamma_2}(\gamma_2) = \sum_{k=1}^{m} \sum_{l=n-m}^{(n+m-2k)k} \frac{c_{kl} \gamma_2^l}{\Gamma(l+1)} \left(\frac{k}{\alpha_{rd}}\right)^{l+1} e^{-\frac{k}{\alpha_{rd}}\gamma_2}. \tag{31}$$

2) Outage Probability of γ_2: Similar to the derivation of the outage probability for the SINR in III.A2 for the first hop, we can use the definition $P_{\text{out}}(\gamma_{th}) \triangleq Pr\left\{\gamma_2 \le \gamma_{th}\right\} = \int_0^{\gamma_{th}} p_{\gamma_2}(\gamma_2) d\gamma_2$, and apply the solution for this integration as $\gamma(n,x) = \int_0^x r^{n-1} e^{-r} dr = \Gamma(n)\left(1 - e^{-x}\sum_{k=0}^{n-1}\left(x^k/k!\right)\right)$ for positive integers n, to obtain the outage probability as

$$\begin{aligned}P_{\text{out2}}(\gamma_{th}) = \sum_{k=1}^{m} \sum_{l=n-m}^{(n+m-2k)k} c_{kl} \left(\frac{k}{\alpha_{rd}}\right) \Bigg[1 - e^{-\frac{k\gamma_{th}}{\alpha_{rd}}} \\ \times \sum_{r=o}^{l} \frac{1}{\Gamma(r+1)} \left(\frac{k\gamma_{th}}{\alpha_{rd}}\right)^r\Bigg]. \end{aligned} \tag{32}$$

3) ASER for M-PSK Modulation Scheme for 2nd Hop: In order to obtain the ASER of the second hop, we can utilize directly (22), for γ_2, along with (31), and utilizing the Q-function instead of $P_e(\gamma_2)$, i.e., $P_e(\gamma_2) = aQ(\sqrt{2g\gamma_2})$, as defined previously in III.A3, to obtain

$$\begin{aligned}\bar{P}_{e2}(\gamma_2) = \sum_{k=1}^{m} \sum_{l=n-m}^{(n+m-2k)k} \frac{c_{kl}\, a}{\Gamma(l+1)} \left(\frac{k}{\alpha_{rd}}\right)^{l+1} \\ \times \int_{\gamma_2=0}^{\infty} \gamma_2^l e^{-\frac{k}{\alpha_{rd}}\gamma_2} Q(\sqrt{2g\gamma_2}) d\gamma_2. \end{aligned} \tag{33}$$

In order to complete the required integration in (33), an alternative formulation of the Q-function known as

Craig's expression can be utilized, which is given as, $Q\left(\sqrt{2g\gamma_2}\right) = \frac{1}{\pi}\int_0^{\pi/2}\exp\left(\frac{-2\,g\,\gamma_2}{2\,\sin^2\theta}\right)d\theta$ [32], and has been solved by ([33], Section 5.4.4). Additionally, by recalling again $\int_0^\infty \gamma^{\nu-1}e^{-\mu\gamma}d\gamma = \mu^{-\nu}\Gamma(\nu)$, and after straightforward mathematical simplifications, we can re-write (33) as

$$\bar{P}_{e2} = \sum_{k=1}^{m}\sum_{l=n-m}^{(n+m-2k)k}\frac{ac_{kl}}{\pi}\int_0^{\frac{\pi}{2}}\left(\frac{\sin^2\theta}{\sin^2\theta+\left(\frac{g\alpha_{rd}}{k}\right)}\right)^{l+1}d\theta, \tag{34}$$

where the integration in (34) can be solved by ([33], 5A.21) to obtain the final expression of $\bar{P}_{e2}$ as

$$\bar{P}_{e2} = \sum_{k=1}^{m}\sum_{l=n-m}^{(n+m-2k)k}\frac{ac_{kl}}{2}\left[1-\sqrt{\frac{R}{1+R}}\times\sum_{r=0}^{l}\binom{2r}{r}\frac{1}{(4+4R)^r}\right], \tag{35}$$

where $R = g\alpha_{rd}/k$. Now, after obtaining the outage probabilities and ASER for the first and second hops, we can evaluate the E2E performance for these two metrics by re-calling (3) which is given by [24] as

$$P_{\text{out}}(\gamma_{th}) = P_{\text{out1}}(\gamma_{th}) + P_{\text{out2}}(\gamma_{th}) - 2P_{\text{out1}}(\gamma_{th})P_{\text{out2}}(\gamma_{th}) \tag{36}$$

$$\bar{P}_e(\gamma_1,\gamma_2) = \bar{P}_{e1}(\gamma_1) + \bar{P}_{e2}(\gamma_2) - 2\bar{P}_{e1}(\gamma_1)\bar{P}_{e2}(\gamma_2) \tag{37}$$

IV. End-to-End Capacity

In this section, we derive the E2E capacity of the proposed FD-MRC-MIMO based on EF relaying in the presence of SI. This derivation aims to obtain the upper bound of the mutual information between the source and the destination by assuming perfect channel estimation. We assume that the processing delay in the EF relaying operation can be applied within a symbol duration. i.e., $\mathbf{s}_i[t] = \mathbf{G}_R\,\mathbf{r}[t-1]$, where $\mathbf{s}_i[t]$ is the transmitted signal at the relay output at time instant t and $\mathbf{G}_R = \mathbf{G}_{tx}\mathbf{w}_{tx}^{rd}F\left(\mathbf{w}_{rx}^{sr}\right)^H\mathbf{G}_{rx}$ represents the combination of all stages of the EF relaying operation in Fig. 1. Hence, we can write $\mathbf{s}_i[t]$ as a function of the received signal at the relay input, $\mathbf{r}[t-1]$, defined in (4) to obtain

$$\mathbf{s}_i[t] = \mathbf{G}_R\left(\mathbf{H}_{sr}\mathbf{w}_{tx}^{sr}s_o[t-1] + \mathbf{H}_{rr}\mathbf{s}_i(s_o[t-2]) + \mathbf{n}_R[t-1]\right). \tag{38}$$

At the destination, the received signal, $\mathbf{y}_D$ can be written as

$$\mathbf{y}_D[t] = \mathbf{H}_{rd}\,\mathbf{s}_i[t] + \mathbf{n}_D[t], \tag{39}$$

where $\mathbf{n}_D[t]$ represents the AWGN in the input of the destination. Moreover, MRC combining is applied to $\mathbf{y}_D[t]$ at the destination as $\hat{s}_o[t-1] = \left(\mathbf{w}_{rx}^{rd}\right)^H\mathbf{y}_D[t]$. Hence, $\hat{s}_o[t-1]$ can be written as

$$\hat{s}_o[t-1] = \left(\mathbf{w}_{rx}^{rd}\right)^H\mathbf{H}_{rd}\,\mathbf{s}_i[t] + \left(\mathbf{w}_{rx}^{rd}\right)^H\mathbf{n}_D[t]. \tag{40}$$

At the moment, by substituting (38) in (40) we can obtain

$$\begin{aligned}\hat{s}_o[t-1] &= (\mathbf{w}_{rx}^{rd})^H\mathbf{H}_{rd}\mathbf{G}_R\left(\mathbf{H}_{sr}\mathbf{w}_{tx}^{sr}s_o[t-1] + \mathbf{H}_{rr}\mathbf{s}_i[t-2] + \mathbf{n}_R[t-1]\right) + (\mathbf{w}_{rx}^{rd})^H\mathbf{n}_D[t],\\ &= \mathbf{G}_D\mathbf{H}_{sr}\mathbf{w}_{tx}^{sr}s_o[t-1] + \mathbf{G}_D\mathbf{H}_{rr}\mathbf{s}_i[t-2] + \mathbf{G}_D\mathbf{n}_R[t-1] + \left(\mathbf{w}_{rx}^{rd}\right)^H\mathbf{n}_D[t],\end{aligned} \tag{41}$$

where $\mathbf{G}_D = \left(\mathbf{w}_{rx}^{rd}\right)^H\mathbf{H}_{rd}\mathbf{G}_R$ was introduced for simplification. From (41), we can find the E2E mutual information of the proposed system, which can be written as

$$\mathcal{I}(s_o;\hat{s}_o) = \log_2\left|\mathbf{I} + \sigma_{s_o}^2\mathbf{G}_D\mathbf{H}_{sr}\mathbf{w}_{tx}^{sr}\left(\mathbf{w}_{tx}^{sr}\right)^H\mathbf{H}_{sr}^H\mathbf{G}_D^H\mathbf{R}_{nn}^{-1}\right|, \tag{42}$$

where $\sigma_{s_o}^2 \triangleq \mathbb{E}\left\{s_o s_o^*\right\} = \frac{P_{sr}}{N_s}$ is the variance of the transmitted signal at source node, and $\mathbf{R}_{nn}$ represents the overall covariance matrix of SI and the noises in the inputs of the relay and the destination, and it can be defined as

$$\mathbf{R}_{nn} = \mathbf{G}_D\mathbf{H}_{rr}\mathbf{R}_{s_i}\mathbf{H}_{rr}^H\mathbf{G}_D^H + \mathbf{G}_D\mathbf{R}_{n_R}\mathbf{G}_D^H + \left(\mathbf{w}_{rx}^{rd}\right)^H\mathbf{R}_{n_D}\mathbf{w}_{rx}^{rd}, \tag{43}$$

where $\mathbf{R}_{n_R} \triangleq \mathbb{E}\left\{\mathbf{n}_R\mathbf{n}_R^H\right\} = \sigma_{n_R}^2\mathbf{I}^{N_{rx}}$ is covariance matrix of the noise at the input of the relay, while $\mathbf{R}_{n_D} \triangleq \mathbb{E}\left\{\mathbf{n}_D\mathbf{n}_D^H\right\} = \sigma_{n_D}^2\mathbf{I}^{N_D}$ is the covariance matrix of noise at the input of the destination node. Additionally, $\mathbf{R}_{s_i} \triangleq \mathbb{E}\left\{\mathbf{s}_i\mathbf{s}_i^H\right\} = \frac{P_i}{N_{tx}}\mathbf{I}^{N_{tx}} = \sigma_{s_{ef}}^2\mathbf{G}_{rx}\mathbf{w}_{tx}^{rd}\left(\mathbf{w}_{tx}^{rd}\right)^H\mathbf{G}_{rx}^H$, which represents the covariance matrix of the relay's transmitted signal causing SI at its receive input. Finally, $\sigma_{s_{ef}}^2 \triangleq \mathbb{E}\left\{s_{ef}s_{ef}^*\right\}$ is the variance of the equalized signal at the relay.

V. Simulation Results and Discussion

In this section, the E2E performance of FD-MRC-MIMO based EF relaying system after applying SIC is considered. Two configurations of the proposed system $(N_s, N_{rx}, N_{tx}, N_d)$ are considered using, i.e., (2, 2, 2, 2) and (4, 4, 4, 4), respectively. The E2E performance is analyzed and simulated depending on the fact that the impairment of SI impacts on the FD-relay input only due to FD operation, as assumed in this paper, and a mitigation using SIC is applied by taking into account residual SI due to imperfect channel estimation in both desired and interference channels. In addition, the relay-to-destination path is considered a regular MIMO link. Moreover, the channels are considered to be independent flat Rayleigh fading channels. The outage probability of the output SINR, in addition to the exact ASER have been simulated and the obtained results have been analyzed. Also, we assumed that the estimation errors for all channels in this paper are the same, i.e., $\rho = \rho_{sr} = \rho_{rr} = \rho_{rd}$.

Figs. 3 and 4 show respectively the PDFs of the SINR for the first hop, γ_1, for (2, 2, 2, 2) and (4, 4, 4, 4) FD-MRC-MIMO system in the case of perfect channel estimation ($\rho = 1$) and an imperfect channel estimation ($\rho = 0.9$) at $\Omega_{sr} = 10$ dB and for two values of Ω_{rr}, namely 6 and 12 dB. The illustrated PDFs demonstrate that obtaining more precise CSI via increasing the accuracy of channel estimation, results in increased output SINR.

Fig. 5 depicts the E2E outage probability of (2, 2, 2, 2) and (4, 4, 4, 4) FD-MRC-MIMO system as a function of the SINR threshold, γ_{th}, for perfect and imperfect channel estimations, i.e., $\rho = 1$ and $\rho = 0.9$, respectively, and for two cases of residual self-interferences to noise ratio, which are $\Omega_{rr} = 6$ and

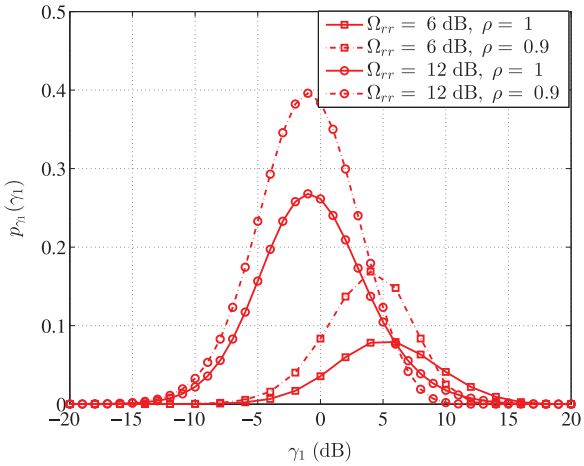

Fig. 3. PDF of the SINR of the first hop for (2, 2, 2, 2) FD-MRC-MIMO after SIC for $\Omega_{sr} = 10$ dB with perfect and imperfect channel estimation in the presence of residual SI with $\Omega_{rr} = 6$ and 12 dB.

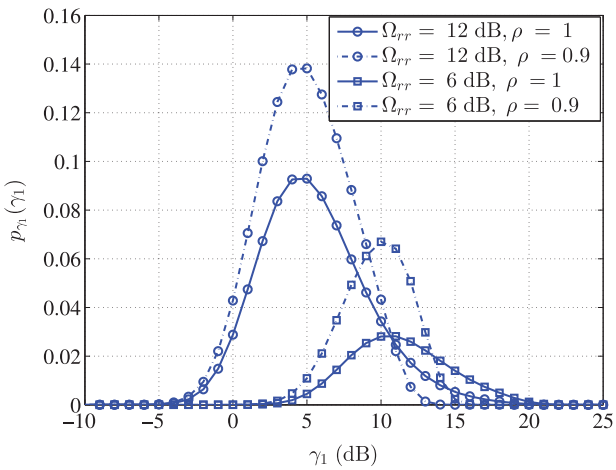

Fig. 4. PDF of the SINR of the first hop for (4, 4, 4, 4) FD-MRC-MIMO after SIC for $\Omega_{sr} = 10$ dB with perfect and imperfect channel estimation in the presence of residual SI with $\Omega_{rr} = 6$ and 12 dB.

12 dB, while the SNR was fixed at $\Omega_{sr} = \Omega_{rd} = 10$ dB. On the other hand, Fig. 6 shows the relationship between the overall E2E outage probability and SNR ($\Omega_{sr} = \Omega_{rd}$), for the same conditions as outlined in Fig. 5, except for the SINR threshold that in this case was fixed at 10 dB. It is evident from the two figures that increasing the number of antennas in FD-MRC-MIMO leads to better performance and enables the system to tolerate more residual SI caused due to channel estimation errors.

Fig. 7 shows the ASER for the system using a quadrature PSK (QPSK) modulation scheme, $(M = 4)$, for the two channel estimation cases and for the two values of SI mentioned previously during this section. Moreover, we compare the analytical results obtained from the derived expression of ASER for QPSK modulation with results obtained via Monte-Carlo simulations as shown in Fig. 8 for a (2, 2, 2, 2) FD-MRC-MIMO system. In this figure, we consider higher Ω_{rr} scenarios ranging between 15 and 30 dB for four cases of channel estimation errors, i.e., $\rho = 0.9, 0.95, 0.99$ and 1. The ASER vs. SNR performance results are obtained by averaging 10^4 frames containing 2048 bits for each SNR point. A closer look at the results shows close

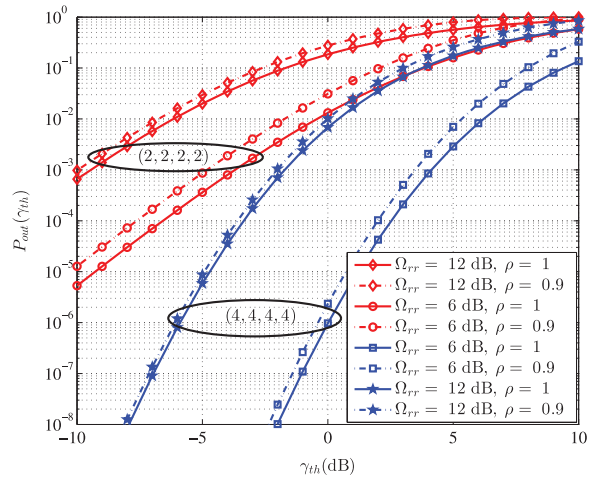

Fig. 5. E2E outage probability of (2, 2, 2, 2) and (4, 4, 4, 4) FD-MRC-MIMO after SIC at $\Omega_{sr} = \Omega_{rd} = 10$ dB and residual $\Omega_{rr} = 6$ and 12 dB with perfect and imperfect channel estimation.

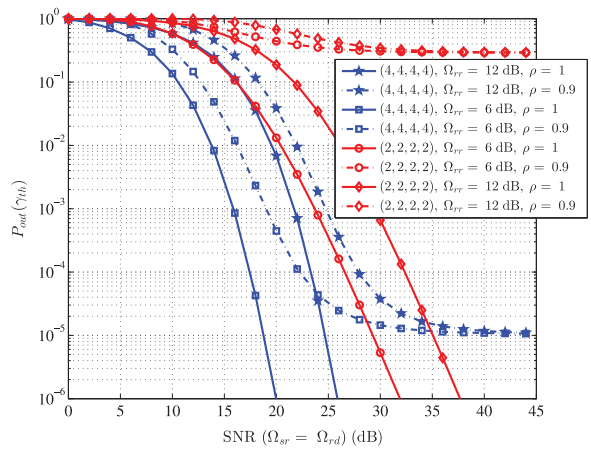

Fig. 6. E2E Outage probability of (2, 2, 2, 2) and (4, 4, 4, 4) FD-MRC-MIMO after SIC at $\gamma_{th} = 10$ dB in the presence of residual SI with $\Omega_{rr} = 6$ and 12 dB.

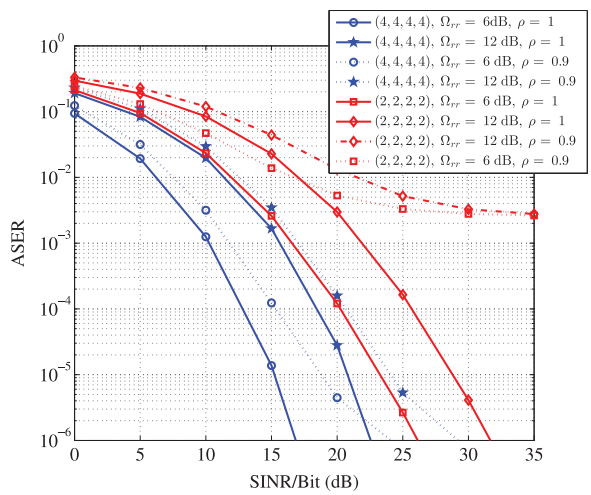

Fig. 7. E2E exact ASER for (2, 2, 2, 2) and (4, 4, 4, 4) FD-MRC-MIMO after SIC for QPSK modulation scheme in the presence of residual SI with $\Omega_{rr} = 6$ and 12 dB.

agreement between simulation and theory. Furthermore, the impact of imperfect channel estimation under higher Ω_{rr} can be

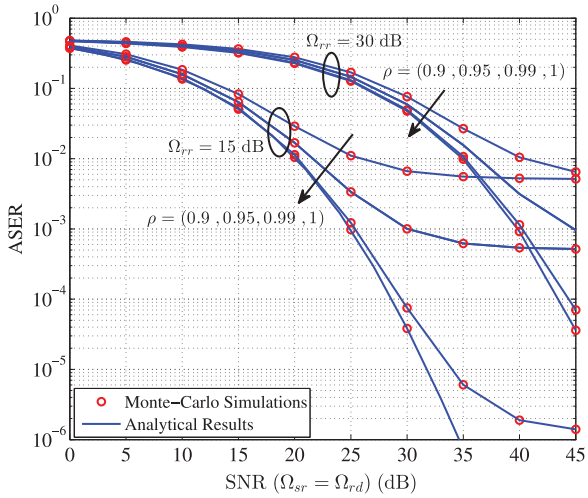

Fig. 8. E2E analytical and Monte-Carlo results of ASER (QPSK modulation) for (2, 2, 2, 2) FD-MRC-MIMO after SIC in the presence of residual SI with $\Omega_{rr} = 15$ and 30 dB and imperfect channel estimation errors of $\rho = (0.9, 0.95, 0.99, 1)$.

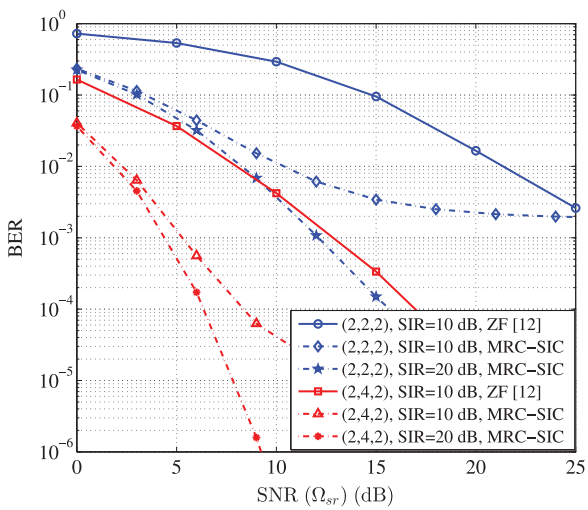

Fig. 9. First hop SNR vs. BER performance for (2, 2, 2) and (2, 4, 2) FD-MRC-MIMO after SIC using QPSK modulation for SIR = 10 and 20 dB at the input of FD relay.

shown in this figure, where the proposed system demonstrates more tolerant and closer achievement to perfect channel estimation at 1% error in CSI. Whilst, by increasing the channels estimation error by 5% and 10%, this causes a deterioration in the performance as expected.

In addition, in Fig. 9, we compare the proposed system with another relevant state-of-the-art NSP technique [12], which utilizes SI suppression using Zero-forcing (ZF) approach for a full-duplex MIMO relay and the results obtained in [12] are for the first hop due to the fact that the first hop is affected by the SI, whilst the second hop represents a regular MIMO link. Fig. 9 demonstrates the BER vs. SNR performance for (N_s, N_{rx}, N_{tx}) as (2, 2, 2) and (2, 4, 2) FD-MRC-MIMO after SIC using QPSK modulation. Two cases of SIR at the input of FD relay are considered, namely SIR $= 10$ dB and 20 dB. It can be observed that the proposed system achieves better performance under the same conditions [12]. This is

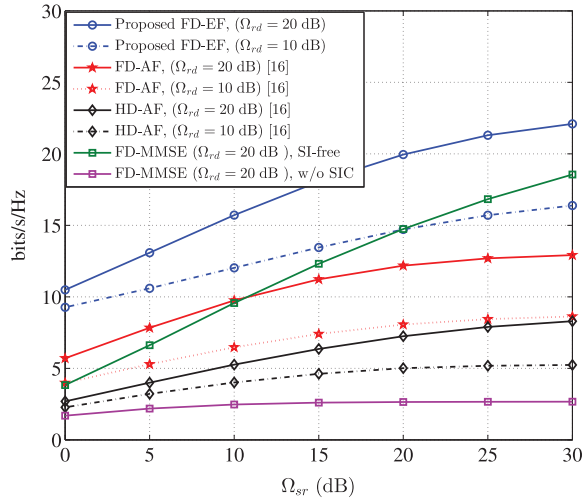

Fig. 10. Average capacity of (2, 2, 2, 2)-FD-MRC-MIMO based EF-ralay, as a function of the mean Ω_{sr} compared to FD-AF, HD-AF and FD-MMSE relays.

due to the exploitation the combination of MRC and SIC for increasing the SNR of the desired signal and also to reduce the INR of the SI respectively, which leads to an increase in SIR. In addition, any further mitigation of SI in the analogue domain, which consequently increases the SIR at the input of the relay, will lead the MRC-SIC system to perform better as shown in the case of SIR $= 20$ dB. For these simulations, the average SNR per bit and average INR per bit are defined as $\Omega_{sr}/\text{bit} = \Omega_{sr}/\log_2(M), \Omega_{rr}/\text{bit} = \Omega_{rr}/\log_2(M)$, and $\Omega_{rd}/\text{bit} = \Omega_{rd}/\log_2(M)$.

Furthermore, in the context of channel capacity, Fig. 10 shows the results obtained from the proposed FD-MRC-MIMO system with (2, 2, 2, 2) as a function of the source-to-relay signal-to-noise ratio, Ω_{sr}, and for two cases of the relay-to-destination signal-to-noise ratio, Ω_{rd}, which are $\Omega_{rd} = 10$ and 20 dB, respectively. A closer look at Fig. 10 reveals that at $\Omega_{sr} = 25$ dB and $\Omega_{rd} = 20$ dB the proposed system achieved average capacity improvements of 9 and 14 bits/s/Hz, respectively, compared to the results obtained by [16] under the same conditions and for the two scenarios of FD-AF and HD-AF. Additionally, we compare the capacity performance of the proposed system for $\Omega_{rd} = 20$ dB as a function of Ω_{sr} with a spatial multiplexing FD full MIMO system with (2, 2, 2, 2) employing MMSE equalization in the relay without NSP. We demonstrate the performance for two scenarios, that of SI-free, and for the case where no SIC is applied. At an $\Omega_{sr} = 25$ dB, a performance gain of approximately 5 and 18 bits/s/Hz is observed, respectively, between the proposed FD-MRC-MIMO and the alternative methods. Finally, Fig. 11 shows the cumulative distribution function (CDF) of the data rate for (2, 2, 2, 2) FD-MRC-MIMO compared to the results obtained by [16] for FD-AF and HD-AF when $\Omega_{sr} = \Omega_{rd} = 20$ dB, in addition to the two scenarios mentioned previously for the spatial multiplexing FD-MIMO system which applying MMSE equalization in the relay and the destination. It worth noting that the CDF was obtained by averaging the mutual information for multiple E2E transmission frames. Close inspection of the results, demonstrate that under the same conditions the proposed

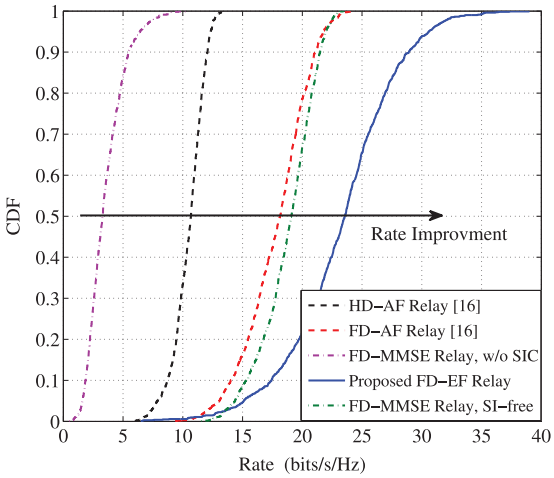

Fig. 11. CDF of the date rate of (2, 2, 2, 2)-FD-MRC-MIMO based EF-ralay, compared to FD-AF, HD-AF and FD-MMSE relays at $\Omega_{sr} = \Omega_{rd} = 20$ dB.

system outperforms, in terms of throughput, the approaches mentioned previously.

VI. Conclusion

In this paper, performance analysis for the proposed FD-MIMO-MRC relay has been presented. The proposed relay combines the MRC technique for increasing the SNR for the desired signal and additionally utilizes SIC to mitigate the SI due to the FD relay operation. The structure of the designed system was outlined using SVD, which was employed in order to cancel the SI via the NSP method. Analytical solutions for the SINR distribution and outage probability have been derived and evaluated. Moreover, the ASER for M-PSK modulation schemes has been derived and computed for QPSK. From the results presented, it is evident that obtaining precise CSI and increasing the number of antennas in FD-MIMO-MRC, especially increasing the antennas at the receiving side of the FD-MIMO relay, leads to better performance and enables the system to tolerate more residual SI caused due to CSI estimation errors. Moreover, it is obvious that increasing the SIR at the input of a FD-MIMO transceiver by applying passive SI mitigation in the analog domain leads to a further increase in performance of the proposed MRC-SIC system. Furthermore, the coefficients of the transformation filter of the EF-relay have been derived to minimize the MSE between the transmitted and the received symbols in the source-relay path, which consequently enhances the system performance in the ASER-SNR metric. In addition, we derive the upper bound of the E2E channel capacity of the proposed system in the presence of SI. The results showed a significant enhancement of the overall throughput. Finally, comparison of the proposed FD-MRC-MIMO approach with another relevant state-of-the-art method was presented demonstrating a considerable performance improvement due to the combination of MRC and SIC techniques in the proposed FD-MRC-MIMO system.

Appendix A
Average SER of the First Hop

By recalling (16)–(18) along with (22) we can obtain

$$\bar{P}_{e1} = \sum_{k=1}^{m} \sum_{l=n-m}^{(n+m-2k)k} \frac{a\, c_{kl}}{\beta} \int_{x=0}^{\infty} e^{\frac{-x}{\beta}} \tag{44}$$

$$\times\, \mathcal{J}\left(2g, \frac{k\,(1+x)}{\alpha_{sr}}, l+1\right) dx, \tag{45}$$

where $\mathcal{J}(\,.\,,\,.\,,\,.\,)$ is defined as

$$\mathcal{J}\left(2g, \frac{k\,(1+x)}{\alpha_{sr}}, l+1\right) = \frac{1}{\Gamma(l+1)} \left(\frac{k(1+x)}{\alpha_{sr}}\right)^{l+1} \tag{46}$$

$$\times \int_{\gamma=0}^{\infty} Q\left(\sqrt{2g\gamma}\right) \exp\left(\frac{-k(1+x)\gamma}{\alpha_{sr}}\right) \gamma^{l}\, d\gamma. \tag{47}$$

At this point, in order to complete the required integrations in (44) and (46), an alternative formulation of the Q-function known as Craig's expression needs to be utilized, which is given as, $Q\left(\sqrt{2g\gamma}\right) = \frac{1}{\pi}\int_0^{\pi/2} \exp\left(\frac{-2\,g\,\gamma}{2\,\sin^2\theta}\right) d\theta$ [32]. Additionally, by recalling again $\int_0^{\infty} \gamma^{\nu-1} e^{-\mu\gamma} d\gamma = \mu^{-\nu}\Gamma(\nu)$ and after straightforward mathematical manipulations, we can re-write (50), as

$$\bar{P}_{e1} = \sum_{k=1}^{m} \sum_{l=n-m}^{(n+m-2k)k} \frac{a\, c_{kl}}{\beta} \int_{x=0}^{\infty} e^{\frac{-x}{\beta}} \tag{48}$$

$$\times\, \mathcal{I}\left(\pi/2\,,\ \frac{g\alpha_{sr}}{k(x+1)}\ ,\ l+1\right) dx, \tag{49}$$

where $\mathcal{I}(\,.\,,\,.\,,\,.\,)$ is defined in (50) and it has been solved in ([33], Section 5.4.4) as

$$\mathcal{I}\left(\frac{\pi}{2}, \frac{g\alpha_{sr}}{k(x+1)}, l+1\right) = \frac{1}{\pi}\int_0^{\pi/2} \left(\frac{\sin^2\theta}{\sin^2\theta + \frac{g\alpha_{sr}}{k(x+1)}}\right)^{l+1} d\theta,$$

$$= \frac{1}{2} - \frac{\sqrt{g\alpha_{sr}/k}}{2} \sum_{r=0}^{l} \sum_{s=0}^{r} U_{rs}\, x^{s} \left(\frac{1}{1+(g\alpha_{sr}/k)+x}\right)^{r+\frac{1}{2}}, \tag{50}$$

where $U_{sr} = \binom{2r}{r}\binom{r}{s}\left(\frac{1}{4}\right)^{r}$. In order to complete the integration of (48), we proceed by identifying the confluent hypergeometric function of the second kind embedded within (48). This function is defined by ([30], (9.211.4)) as

$$\Psi(a;b;z) = \frac{1}{\Gamma(a)} \int_0^{\infty} e^{-zx}\ x^{a-1}(1+x)^{b-a-1} dx. \tag{51}$$

The average SER can be then obtained for several modulation schemes by choosing the appropriate digital modulation constants a and g as

$$\bar{P}_{e1} = \sum_{k=1}^{m} \sum_{l=n-m}^{(n+m-2k)k} \frac{a\, c_{kl}}{2} \left[1 - \left(\frac{g\alpha_{sr}}{k}\right)^{\frac{1}{2}} \frac{1}{\beta} \sum_{r=0}^{l} \sum_{s=0}^{r} \right.$$

$$\times \binom{2r}{r}\binom{r}{s}\left(\frac{1}{4}\right)^{r} \Gamma(s+1)\left(1+\frac{g\alpha_{sr}}{k}\right)^{(s-r+\frac{1}{2})}$$

$$\left. \times \Psi\left(s+1; s-r+\frac{3}{2}; \frac{1}{\beta}\left(1+\frac{g\alpha_{sr}}{k}\right)\right)\right]. \tag{52}$$

The confluent hypergeometric function can be solved using the generalized hypergeometric function either by (53) ([30], (9.210.2)), or (54) ([34], Eq. (6.6.1)) for positive values of a and z, i.e.,

$$\Psi(a;b;z) = \frac{\pi}{\sin(\pi b)}\left[\frac{{}_1F_1(a;b;z)}{\Gamma(a-b+1)\Gamma(b)} - \frac{z^{1-b}\,{}_1F_1(a-b+1;2-b;z)}{\Gamma(a)\Gamma(2-b)}\right], \quad (53)$$

$$\Psi(a;b;z) = z^{-a}\,{}_2F_0\left(a, 1+a-b; \quad ; -z^{-1}\right). \quad (54)$$

Appendix B
Linear MMSE Equalizer

In this Appendix, we will derive the coefficient F of the proposed EF relay, the results in MMSE between the transmitted symbols of the source node $s_o[t]$ and the equalized symbols in the relay $s_{ef}[t]$. From Fig. 1, we can express the symbol at the input of the equalization stage $\tilde{z}[t]$ as

$$\tilde{z}[t] = \left(\mathbf{w}_{rx}^{sr}\right)^H \mathbf{G}_{rx}\left[\mathbf{H}_{sr}\mathbf{w}_{tx}^{sr}s_o[t] + \mathbf{H}_{rr}\mathbf{s}_i[t] + \mathbf{n}_R[t]\right], \quad (55)$$

while the tth symbol at the out of the equalization stage $s_{ef}[t]$ can be evaluated as $s_{ef} = F\,\tilde{z}[t]$, which can be re-written using (55) as

$$s_{ef}[t] = F\left(\mathbf{w}_{rx}^{sr}\right)^H \mathbf{G}_{rx}\mathbf{H}_{sr}\mathbf{w}_{tx}^{sr}s_o[t] + F\left(\mathbf{w}_{rx}^{sr}\right)^H \mathbf{G}_{rx}\mathbf{H}_{rr}\mathbf{s}_i[t] + F\left(\mathbf{w}_{rx}^{sr}\right)^H \mathbf{G}_{rx}\mathbf{n}_R[t]. \quad (56)$$

Now, we can define MSE, $\mathrm{MSE}(F)$, between the transmitted symbol, $s_o[t]$, and the equalized symbol, $s_{ef}[t]$, as

$$\mathrm{MSE}(F) \triangleq \mathbb{E}\left\{(s_o[t] - s_{ef}[t])(s_o[t] - s_{ef}[t])^*\right\}. \quad (57)$$

From (56), and after some manipulation and simplification steps, (57) becomes

$$\mathrm{MSE}(F) = F\left[\sigma_{s_o}^2 h_o h_o^* + \sigma_{s_{ef}}^2 h_I h_I^* + \overline{R}_{n_R}\right]F^* - \quad h_o^*F^* - h_I^*F^*, \quad (58)$$

with

$$h_o = \left(\mathbf{w}_{rx}^{sr}\right)^H \mathbf{G}_{rx}\mathbf{H}_{sr}\mathbf{w}_{tx}^{sr}, \quad (59a)$$

$$h_I = \left(\mathbf{w}_{rx}^{sr}\right)^H \mathbf{G}_{rx}\mathbf{H}_{rr}\mathbf{G}_{rx} \quad (59b)$$

$$\overline{R}_{n_R} = \left(\mathbf{w}_{rx}^{sr}\right)^H \mathbf{G}_{rx}\mathbf{R}_{n_R}\mathbf{G}_{rx}^H\mathbf{w}_{rx}^{sr}. \quad (59c)$$

Following to the derivations in [35], [36], this MSE function is a convex function of F^*, therefore, the optimum value of F, which represents the MMSE between $s_o[t]$ and $s_{ef}[t]$, can be obtained by applying a differentiation to (58) with respect to F^* and equating the result to zero. Thus, the transformation coefficient of the EF-relay, F, can be obtained in exact form as

$$F = \left[\sigma_{s_o}^2 h_o h_o^* + \sigma_{s_{ef}}^2 h_I h_I^* + \overline{R}_{n_R}\right]^{-1}(h_o^* + h_I^*) \quad (60)$$

Acknowledgment

The authors would like to thank the Research Council for funding. No new data were created during this study.

References

[1] T. Riihonen and R. Wichman, "Analog and digital self-interference cancellation in full-duplex MIMO-OFDM transceivers with limited resolution in A/D conversion," in *Proc. 46th Asilomar Conf. Signals. Syst.*, Nov. 2012, pp. 45–49.
[2] T. Riihonen, S. Werner, and R. Wichman, "Mitigation of loopback self-interference in full-duplex MIMO relays," *IEEE Trans. Signal Process.*, vol. 59, no. 12, pp. 5983–5993, Dec. 2011.
[3] K. Haneda, E. Kahra, S. Wyne, C. Icheln, and P. Vainikainen, "Measurement of loop-back interference channels for outdoor-to-indoor full-duplex radio relays," in *Proc. 4th Eur. Conf. Antennas Propag. (EuCAP)*, Apr. 2010, pp. 1–5.
[4] M. Khojastepour and S. Rangarajan, "Wideband digital cancellation for full-duplex communications," in *Proc. 46th Asilomar Conf. Signals, Syst. Comput.*, Nov. 2012, pp. 1300–1304.
[5] B. Day, A. Margetts, D. Bliss, and P. Schniter, "Full-duplex MIMO relaying: Achievable rates under limited dynamic range," *IEEE J. Sel. Areas Commun.*, vol. 30, no. 8, pp. 1541–1553, Sep. 2012.
[6] B. Day, D. Bliss, A. Margetts, and P. Schniter, "Full-duplex bidirectional MIMO: Achievable rates under limited dynamic range," in *Proc. 45th Asilomar Conf. Signals, Syst. Comput.*, Nov. 2011, pp. 1386–1390.
[7] T. Riihonen, A. Balakrishnan, K. Haneda, S. Wyne, S. Werner, and R. Wichman, "Optimal eigenbeamforming for suppressing self-interference in full-duplex MIMO relays," in *Proc. 45th Ann. Conf. Inf. Sci. Syst. (CISS)*, Mar. 2011, pp. 1–6.
[8] T. Riihonen, S. Werner, and R. Wichman, "Transmit power optimization for multiantenna decode-and-forward relays with loopback self-interference from full-duplex operation," in *Proc. 45th Asilomar Conf. Signals, Syst. Comput.*, Nov. 2011, pp. 1408–1412.
[9] M. Duarte and A. Sabharwal, "Full-duplex wireless communications using off-the-shelf radios: Feasibility and first results," in *Proc. 44th Asilomar Conf. Signals, Syst. Comput.*, Nov. 2010, pp. 1558–1562.
[10] A. Sahai, G. Patel, C. Dick, and A. Sabharwal, "Understanding the impact of phase noise on active cancellation in wireless full-duplex," in *Proc. 46th Asilomar Conf. Signals, Syst. Comput.*, Nov. 2012, pp. 29–33.
[11] T. Riihonen, S. Werner, and R. Wichman, "Residual self-interference in full-duplex MIMO relays after null-space projection and cancellation," in *Proc. 44th Asilomar Conf. Signals, Syst. Comput.*, Nov. 2010, pp. 653–657.
[12] T. Riihonen, S. Werner, and R. Wichman, "Spatial loop interference suppression in full-duplex MIMO relays," in *Proc. 43rd Asilomar Conf. Signals, Syst. Comput.*, Nov. 2009, pp. 1508–1512.
[13] H. Ju, E. Oh, and D. Hong, "Improving efficiency of resource usage in two-hop full duplex relay systems based on resource sharing and interference cancellation," *IEEE Trans. Wireless Commun.*, vol. 8, no. 8, pp. 3933–3938, Aug. 2009.
[14] A. Maaref and S. Aissa, "Closed-form expressions for the outage and ergodic Shannon capacity of MIMO MRC systems," *IEEE Trans. Commun.*, vol. 53, no. 7, pp. 1092–1095, Jul. 2005.
[15] M. Kang and M.-S. Alouini, "A comparative study on the performance of MIMO MRC systems with and without cochannel interference," *IEEE Trans. Commun.*, vol. 52, no. 8, pp. 1417–1425, Aug. 2004.
[16] Y. Y. Kang and J. H. Cho, "Capacity of MIMO wireless channel with full-duplex amplify-and-forward relay," in *Proc. IEEE 20th Int. Symp. Personal, Indoor, Mobile Radio Commun.*, Sep. 2009, pp. 117–121.
[17] T. Riihonen, S. Werner, and R. Wichman, "Comparison of full-duplex and half-duplex modes with a fixed amplify-and-forward relay," in *Proc. IEEE Wireless Commun. Netw. Conf. (WCNC)*, Apr. 2009, pp. 1–5.
[18] O. Munoz-Medina, J. Vidal, and A. Agustin, "Linear transceiver design in nonregenerative relays with channel state information," *IEEE Trans. Signal Process.*, vol. 55, no. 6, pp. 2593–2604, June 2007.
[19] A. Paulraj, R. Nabar, and D. Gore, *Introduction to Space-Time Wireless Communications*. Cambridge, U.K.: Cambridge Univ. Press, 2003.
[20] T. Riihonen, S. Werner, and R. Wichman, "Hybrid full-duplex/half-duplex relaying with transmit power adaptation," *IEEE Trans. Wireless Commun.*, vol. 10, no. 9, pp. 3074–3085, Sept. 2011.
[21] P. Lioliou, M. Viberg, M. Coldrey, and F. Athley, "Self-interference suppression in full-duplex MIMO relays," in *Proc. 44th Asilomar Conf. Signals, Syst. Comput.*, Nov. 2010, pp. 658–662.
[22] D. Kim, H. Ju, S. Park, and D. Hong, "Effects of channel estimation error on full-duplex two-way networks," *IEEE Trans. Veh. Technol.*, vol. 62, no. 9, pp. 4666–4672, Nov. 2013.
[23] H. Ju, S. Lee, K. Kwak, E. Oh, and D. Hong, "A new duplex without loss of data rate and utilizing selection diversity," in *Proc. IEEE Veh. Technol. Conf. (VTC—Spring)*, May 2008, pp. 1519–1523.
[24] M. Hasna and M.-S. Alouini, "End-to-end performance of transmission systems with relays over Rayleigh-fading channels," *IEEE Trans. Wireless Commun.*, vol. 2, no. 6, pp. 1126–1131, 2003.

[25] R. Annavajjala, P. Cosman, and L. Milstein, "Performance analysis of linear modulation schemes with generalized diversity combining on Rayleigh fading channels with noisy channel estimates," *IEEE Trans. Inf. Theory*, vol. 53, no. 12, pp. 4701–4727, 2007.
[26] L. Yang and J. Qin, "Outage performance of MIMO MRC systems with unequal-power co-channel interference," *IEEE Commun. Lett.*, vol. 10, no. 4, pp. 245–247, Apr. 2006.
[27] J. Proakis and M. Salehi, *Digital Communications*. New York, NY, USA: McGraw-Hill, 2008.
[28] S. Ikki and S. Aissa, "Impact of imperfect channel estimation and co-channel interference on regenerative cooperative networks," *IEEE Wireless Commun. Lett.*, vol. 1, no. 5, pp. 436–439, 2012.
[29] P. Dighe, R. Mallik, and S. Jamuar, "Analysis of transmit-receive diversity in Rayleigh fading," in *Proc. IEEE Global Telecommun. Conf. (IEEE GLOBECOM)*, 2001, vol. 2, pp. 1132–1136.
[30] A. Jeffrey and D. Zwillinger, *Table of Integrals, Series, and Products*, ser. Table of Integrals, Series, and Products Series. New York, NY, USA: Elsevier Science, 2007.
[31] Y. Tokgoz and B. Rao, "The effect of imperfect channel estimation on the performance of maximum ratio combining in the presence of cochannel interference," *IEEE Trans. Veh. Technol.*, vol. 55, no. 5, pp. 1527–1534, Sept. 2006.
[32] A. Goldsmith, *Wireless Communications*. New York, NY, USA: Cambridge Univ. Press, 2005.
[33] M. Simon and M. Alouini, *Digital Communication Over Fading Channels: A Unified Approach to Performance Analysis*, ser. Wiley series in telecommunications and signal processing. New York, NY, USA: Wiley, 2000.
[34] H. Bateman and A. Erdelyi, *Higher Transcendental Functions*. New York, NY, USA: McGraw-Hill, 1953, vol. 1.
[35] S. Barbarossa, *Multiantenna Wireless Communications Systems*, ser. Artech House mobile communications library. Norwood, MA, USA: Artech House, 2005.
[36] D. Palomar, J. Cioffi, and M. A. Lagunas, "Joint Tx-Rx beamforming design for multicarrier MIMO channels: A unified framework for convex optimization," *IEEE Trans. Signal Process.*, vol. 51, no. 9, pp. 2381–2401, 2003.

Mohamad A. Ahmed (S'13) obtained his B.Sc. in electrical engineering (electronic and communication) from Mosul University, Mosul, Iraq, in 1999. He received his M.Sc. *with distinction* in communication and signal processing at Newcastle University, U.K., in 2009. He is on study leave from the College of Electronic Engineering, University of Mosul, Iraq. He is currently working toward the Ph.D. degree at the School of Electrical and Electronics Engineering, Newcastle University, Newcastle Upon Tyne, U.K. His research emphasizes on the field of full-duplex-MIMO wireless communications. His current research interests include numerical, simulation, and theoretical performance analyses of this system. Moreover, He is interested in the subjects of digital communications, Microwave, Radio Frequency Engineering, and Digital signal processing.

Charalampos C. Tsimenidis (M'05–SM'12) is a Senior Lecturer in Signal Processing for Communications in the School of Electrical and Electronic Engineering. He received his M.Sc. with distinction and Ph.D. in communications and signal processing from Newcastle University in 1999 and 2002, respectively. His main research interests are in the area of digital communications with focus on full-duplex and massive MIMO systems. During the last 14 years has published over 180 conference and journal papers, supervised successfully 3 M.Phil. and 29 Ph.D. Students and made contributions in the area of transceiver design to several European and U.K. funded research projects.

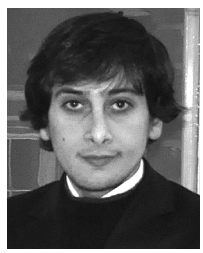

Anas F. Al Rawi (S'08–M'13) received his M.Sc. (with distinction) and Ph.D. degrees in communications and signal processing from Newcastle University, U.K., in 2007 and 2011, respectively. From 2010 to 2012, he joined the school of electrical and electronic engineering of Swansea University, Swansea, United Kingdom, as a postdoctoral researcher. In 2012, he was a research associate in the institute of electronics, communications and information technology of Queen's University of Belfast, Belfast, United Kingdom. Currently, Anas is a senior researcher with the Access Network Research team, Research and Technology, BT, Adastral Park, Martlesham, United Kingdom. His primary role focuses on the modelling of the current wireline technologies and its future generations. His research interests include computational electromagnetics, transmission cross-layer optimization, cooperative networks and multi-mode MIMO systems modelling.